AD-A170 201 NONLINEAR WAVE PROPAGATION STUDY(U) ROCKWELL 1/1
INTERNATIONAL THOUSAND OAKS CA SCIENCE CENTER
J R BULAU ET AL. APR 86 SC5361-10FR AFOSR-TR-86-0497
UNCLASSIFIED F49620-83-C-0065 F/G 8/7 NL

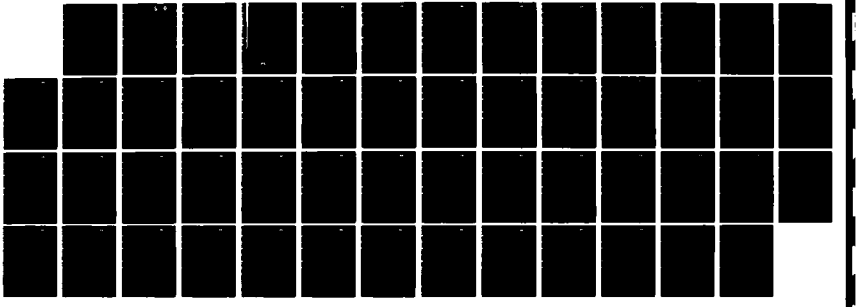

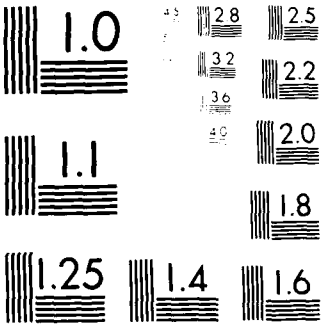

(2)

AD-A170 201

REPORT DOCUMENTATION PAGE

Unclassified	1b. RESTRICTIVE MARKINGS
2a. SECURITY CLASSIFICATION AUTHORITY	3. DISTRIBUTION/AVAILABILITY OF REPORT: Approved for public release; distribution unlimited.
2b. DECLASSIFICATION/DOWNGRADING SCHEDULE	
4. PERFORMING ORGANIZATION REPORT NUMBER(S): SC5361.10FR	5. MONITORING ORGANIZATION REPORT NUMBER(S)
6a. NAME OF PERFORMING ORGANIZATION: Rockwell International Science Center	6b. OFFICE SYMBOL (If applicable)
6c. ADDRESS (City, State and ZIP Code): 1049 Camino Dos Rios, Thousand Oaks, CA 91360	7a. NAME OF MONITORING ORGANIZATION: Air Force Office of Scientific Research, Directorate of Physical and Geophysical Sciences
	7b. ADDRESS (City, State and ZIP Code): Building 410, Bolling AFB, DC 20332
8a. NAME OF FUNDING/SPONSORING ORGANIZATION: Defense Advanced Research Projects Agency	8b. OFFICE SYMBOL (If applicable): NP
8c. ADDRESS (City, State and ZIP Code): 1400 Wilson Blvd Bldg 410, Bolling AFB DC 20332-6448	9. PROCUREMENT INSTRUMENT IDENTIFICATION NUMBER: Contract No. F49620-83-C-0065
11. TITLE (Include Security Classification): NONLINEAR WAVE PROPAGATION STUDY (U)	10. SOURCE OF FUNDING NOS: PROGRAM ELEMENT NO: 61102F; PROJECT NO: 2309; TASK NO: A2; WORK UNIT NO: N/A
12. PERSONAL AUTHOR(S): Tittmann, B.R. and Bulau, J.R.	
13a. TYPE OF REPORT: Final Report	13b. TIME COVERED: FROM 05/01/83 TO 10/30/85
14. DATE OF REPORT (Yr., Mo., Day): APRIL 1986	15. PAGE COUNT: 50
16. SUPPLEMENTARY NOTATION: The views and conclusions contained in this document are those of the authors and should not be interpreted as necessarily representing the official policies, either expressed or implied, of the Defense Advanced Research Projects Agency of the U.S. Government.	

17 COSATI CODES			18 SUBJECT TERMS (Continue on reverse if necessary and identify by block number)
FIELD	GROUP	SUB GR	

19 ABSTRACT (Continue on reverse if necessary and identify by block number)

We have examined some of the methods available for use in the laboratory to measure the inelastic attenuation of seismic waves in rocks. We conclude that the forced swept resonance technique is best suited for measuring the Q of linear anelastic materials, and for defining the transition amplitude from linear anelastic behavior to nonlinear behavior. For evaluating losses in materials at high amplitudes, which exceed the elastic limit, the best technique requires simultaneous measurements of the time functions of stress and strain under conditions that simulate seismic loading as closely as possible.

We have also studied the transition region from linearity to nonlinearity in a test specimen of Westerly granite at elevated effective pressures using the mechanical resonance approach. Nonlinear effects, both in flexure and in shear, are observed when the strain exceeds 10^{-6}, increasing slightly with increasing effective pressure. These transition amplitudes probably represent lower limits on the amplitude of transition from linear to nonlinear behavior for a compressional pulse propagating through the near-fields of an explosion.

The details of stress-strain hysteresis loops have been examined for a number of different rock specimens using

20 DISTRIBUTION/AVAILABILITY OF ABSTRACT: UNCLASSIFIED/UNLIMITED ☒ SAME AS RPT ☐ DTIC USERS ☐	21 ABSTRACT SECURITY CLASSIFICATION: Unclassified
22a NAME OF RESPONSIBLE INDIVIDUAL: JOHN F. PRINCE	22b TELEPHONE NUMBER (Include Area Code): 202/767-4908
	22c OFFICE SYMBOL: NP

DD FORM 1473, 83 APR EDITION OF 1 JAN 73 IS OBSOLETE

UNCLASSIFIED
SECURITY CLASSIFICATION OF THIS PAGE

(Block 19 continued)

alternating compressive and tensile stresses. Our experimental results support the following general observations: (1) rocks have a larger effective modulus in compression than in tension; (2) most of the energy lost during a full cycle of loading occurs as a result of strain in extension, since the hysteresis loops are smaller in compression than in tension; (3) stress-strain hysteresis loop traces appear to be independent of frequency. These observations indicate a loss mechanism associated with intergranular friction. In compression, intergranular sliding is apparently restricted by the impingement of opposing crack faces, while in tension this does not occur. Thus, laboratory measurements of attenuation that use alternating compressive and tensile loads may overestimate the attenuation of high amplitude compressive waves with the same maximum strain.

SC5361.10FR

SC5361.10FR

Copy No. ____

NONLINEAR WAVE PROPAGATION STUDY

FINAL REPORT FOR THE PERIOD
May 1, 1983 through October 30, 1985

CONTRACT NO. F49620-83-C-0065
DARPA ORDER NO. 4400
PROGRAM CODE: 3A10

Prepared for

Air Force Office of Scientific Research
Building 410
Bolling AFB, DC 20332

Prepared by

J.R. Bulau
805-373-4153
and
B.R. Tittmann

Sponsored by

Defense Advanced Research Projects Agency (DoD)
DARPA Order No. 4400
Monitored by NP Under Contract No. F49620-83-C-0065

Rockwell International
Science Center

TABLE OF CONTENTS

LIST OF FIGURES

LIST OF FIGURES

LIST OF FIGURES

LIST OF FIGURES

LIST OF FIGURES

LIST OF TABLES

1.0 SUMMARY

We have examined some of the methods available for use in the laboratory to measure the inelastic attenuation of seismic waves in rocks. We conclude that the forced swept resonance technique is best suited for measuring the Q of linear anelastic materials, and for defining the transition amplitude from linear anelastic behavior to nonlinear behavior. For evaluating losses in materials at high amplitudes, which exceed the elastic limit, the best technique requires simultaneous measurements of the time functions of stress and strain under conditions that simulate seismic loading as closely as possible.

We have also studied the transition region from linearity to nonlinearity in a test specimen of Westerly granite at elevated effective pressures using the mechanical resonance approach. Nonlinear effects, both in flexure and in shear, are observed when the strain exceeds 10^{-6}, increasing slightly with increasing effective pressure. These transition amplitudes probably represent lower limits on the amplitude of transition from linear to nonlinear behavior for a compressional pulse propagating through the near-fields of an explosion.

The details of stress-strain hysteresis loops have been examined for a number of different rock specimens using alternating compressive and tensile stresses. Our experimental results support the following general observations: (1) rocks have a larger effective modulus in compression than in tension; (2) most of the energy lost during a full cycle of loading occurs as a result of strain in extension, since the hysteresis loops are smaller in compression than in tension; (3) stress-strain hysteresis loop traces appear to be independent of frequency. These observations indicate a loss mechanism associated with intergranular friction. In compression, intergranular sliding is apparently restricted by the impingement of opposing crack faces, while in tension this does not occur. Thus, laboratory measurements of attenuation that use alternating compressive and tensile loads may overestimate the attenuation of high amplitude compressive waves with the same maximum strain.

2.0 INTRODUCTION

The mechanics of wave propagation through the near field of an explosive seismic source are not completely understood, particularly in the peak strain amplitude range between 10^{-4} and 10^{-6}. The most complete data sets that describe free-field wave propagation as a function of scaled distance (distance/yield$^{1/3}$) in this strain amplitude range have been obtained for explosions in polycrystalline salt. The data base includes measurements from (a) the 5.3 kT nuclear event, SALMON (Perret, 1967; Trulio, 1978); (b) the medium to large scale chemical explosions of the COWBOY experiments, which took place in a natural salt dome (Trulio, 1978, 1981); and (c) a series of small scale chemical explosions in pressed polycrystalline salt in the laboratory (Larson, 1982). When all available data are combined, it appears that wave propagation satisfies cube root of yield scaling. That is, the decay of peak particle velocity and displacement can be defined as a function of distance/yield$^{1/3}$ (Trulio, 1978, 1981; Larson, 1982). This appears to be the case, even though available data cover approximately 10 decades in yield, 4 decades in peak particle velocity, and 4 decades in frequency. However, the data fit a line that decays much faster than r^{-1}, which should be the case if the material behaves in a perfectly elastic manner. Thus, the behavior of salt in the range of available free field measurements, to strains as low as approximately 7×10^{-6}, cannot be regarded as perfectly elastic (Trulio, 1978, 1981). Because of the uncertainties regarding the amount of energy that can be dissipated as a seismic pulse propagates at intermediate strains, Bache, et al (1981) have questioned the usefulness of reduced displacement potential (RDP) calculations based on close range data for the purpose of defining a seismic source function.

The exact nature of attenuation in the near field of an explosive seismic source remains a controversial subject. In fact, the evidence regarding the issue of linearity vs nonlinearity appears to be a bit ambiguous. Larson (1982) measured a Q of 12.5 near 10^{-3} strain, and a Q of 24.9 near 6×10^{-4} strain, in the laboratory using small scale chemical explosions in pressed salt. The fact that Q is amplitude dependent is evidence for nonlinear response. However, Larson also demonstrated an approximately linear superposition of wave-

forms at strains higher than 10^{-4}, which suggests near-linearity. The experimental results reported in Tittmann (1983) using resonating bars of natural halite indicate that the linear anelastic Q of halite is quite high, near 500, with a transition to an amplitude dependent nonlinear Q at strain amplitudes greater than approximately 2×10^{-6}. Burdick, et al. (1984a) have argued that it is possible to model a seismic source function for the Amchitka tests, detonated in volcanic material, assuming linear behavior in the near field just outside the spall zone ($\sim$ 700-1200 $m/kT^{1/3}$). Furthermore, Burdick, et al (1984b) contend that the same model can be used to predict the first vertical pulse arrival and rise times even within the spall zone. They used the concept of a compressional elastic radius, which in fact may be considerably smaller than a tensional elastic radius, and which must extend at least as far as the outer limits of the spall zone. Minster and Day (1985) recently re-examined the COWBOY data set, and concluded that it is possible to explain simultaneously the radial decay of peak displacement and peak velocity by either (a) a linear anelastic model with low Q ($\sim$ 20) or (b) a nonlinear model with amplitude-dependent Q. MacCarter and Wortman (1985) conclude that the free-field motion measurements from the SALMON event are consistent with an amplitude-independent Q of about 10. In any case, these amplitude-independent Q values are too low to represent the linear anelastic Q of salt according to the results of Tittmann (1983).

In a more recent study of explosive-induced wave propagation in Nugget sandstone, Larson (1984) reported Q measurements between 8 and 20 at strains between 2×10^{-4} and 2×10^{-2}. Although low strain ($< 10^{-6}$) attenuation measurements are not available for Nugget sandstone, Tittmann et al (1981) and Winkler et al (1979) report relatively high Q values (> 100) for dry Berea and Boise sandstones under linear conditions.

While generally it is acknowledged that Q is defined rigorously only when the material through which a wave propagates behaves linearly, it is common (McCarter and Wortman, 1985; Minster and Day, 1985) to assume for theoretical purposes that "nonlinear Q" can be defined using the equations of Mavko (1979) and Stewart, et al (1983):

$$Q^{-1}(\omega,\varepsilon) = Q_0^{-1}(\omega) + \alpha\varepsilon \qquad (1)$$

where Q^{-1} is nonlinear attenuation, Q_0^{-1} is linear anelastic attenuation, ω is frequency, α is a constant, and ε is strain. This equation considers the combined effects of Coulomb-type friction from many intergranular contacts on the energy dissipated during one full elastic wave cycle. In their derivations, Q^{-1} was defined as

$$Q^{-1} = (1/2\ \pi)(\Delta W/W) \qquad (2)$$

where ΔW is the energy dissipated in one full cycle, and W is the peak strain energy stored per cycle.

One technique used in the laboratory to estimate nonlinear Q involves the forced resonance of bars. The resonating bar approach offers a particularly sensitive tool for detecting the onset of nonlinearity, even at very low strains. The data reported by Tittmann (1983) indicate that the intrinsic linear attenuation of dome salt is quite low ($Q > 500$), and that the onset for nonlinear behavior is near 2×10^{-6} strain, corresponding to approximately 1 bar of stress. Similar behavior has been reported for other rock types, including granite, limestones, sandstones, and miscellaneous igneous rocks (cf Mavko, 1979; Stewart et al, 1983). These measurements suggest that nonlinear response should persist to large scaled distances from explosions, on the order of 10^4 m/kt$^{1/3}$. Furthermore, the low Q values calculated by Larson (1982) [laboratory measurements], Trulio (1979, 1981) [COWBOY], Minster and Day (1985) [COWBOY] and McCarter and Wortman (1985) [COWBOY, SALMON] from free-field measurements in salt are much lower. This constitutes additional evidence of nonlinearity in available free-field measurements.

The experimental results obtained in the previous program (Tittmann, 1983) indicate that natural dome salt is rather ideally behaved. Linear anelastic behavior is indicated when (1) the attenuation and resonant frequency are independent of vibration amplitude and (2) a proportionality exists between driving voltage and vibration amplitude. At elevated effective pressures linear anelastic behavior is observed at strain amplitudes below about 2×10^{-6}, corre-

sponding to stresses of about 1 bar. The linear anelastic Q for a dry natural dome salt specimen was quite high (~ 500 in extension and ~ 1000 in torsion), apparently independent of pressure up to 6.8×10^7 Pa, and very slightly dependent on frequency between ~ 80 Hz and ~ 480 Hz. Nonlinear behavior, as reflected in an amplitude-dependent Q, was observed at strain amplitudes above 2×10^{-6}, at all effective pressures to 6.8×10^7 Pa (corresponding to burial depths of ~ 2.4 km). The behavior of pressed salt contrasted with that of natural dome salt. Weakly nonlinear behavior persisted to very low amplitudes (below 10^{-8}), corresponding to stresses of approximately 0.01 bars. Strongly nonlinear behavior is observed at strain amplitudes higher than 10^{-6}. Under ambient pressure conditions attenuation in pressed salt was sensitive to the amount of moisture adsorbed either on the surface or within the interior of the specimen.

The previous study (Tittmann, 1983) raised a number of questions regarding the experimental methods used to measure nonlinear Q, and to parameterize the nonlinear inelastic properties of rocks. Solutions to some of these issues were explored in this program and are contained in this report.

3.0 Q AND MODULUS MEASUREMENT TECHNIQUES

3.1 Resonance Methods

3.1.1 Linear Regime

Several of the issues addressed in tnis report relate to using resonating bar measurements for estimating P- and S-wave velocity. The resonance measurements are normally carried out with relatively thin, inertially loaded specimens and involve Q and modulus measurements corresponding to at least two modes of vibration: flexure or extension, and torsion. Calculations of seismic body wave properties from laboratory measurements are reasonably good provided that (1) the resonator is properly designed and constructed, and (2) the response of the specimen to loading is macroscopically homogeneous.

The apparatus which was used in the previous program (Tittmann, 1983) has also been used for parts of this study. It is illustrated schematically in Fig. 3.1. This apparatus is used to generate vibrations and to measure their amplitude in both flexure and torsion. Its design has evolved from earlier models to include the following features which are essential for obtaining reliable measurements of modulus and attenuation: (1) a very stiff clamp-arm-rotor assembly designed to minimize bending moments in any part of the apparatus other than the test specimen, (2) rigid mechanical coupling between the test sample and the rest of the resonator assembly, and (3) minimal internal friction within the apparatus itself during sample resonance. The resonator has been designed to minimize instrumental corrections. However, careful measurements have been performed using low dissipation standards with known modulus in order to quantify instrumental/system factors, such as aerodynamic drag, which must be incorporated into modulus and attenuation calculations.

3.1.2 Nonlinear Regime

Although the resonant bar-type measurements are well suited for measuring attenuation and modulus in the linear anelastic regime, and for defining the transition from linear to nonlinear behavior, several other issues need to be

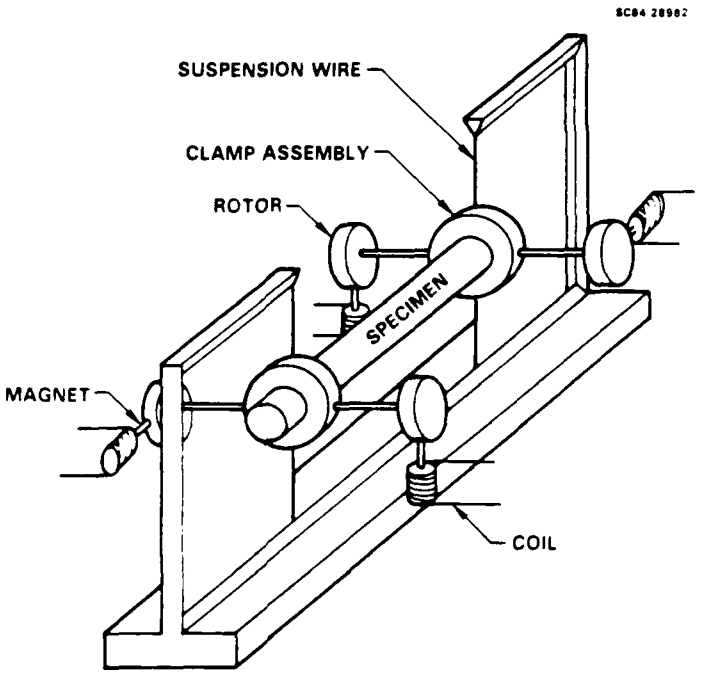

Fig. 3.1 Schematic illustration of the resonant bar apparatus used for studies of dynamic modulus and attenuation as a function of strain amplitude.

considered before one can apply the high amplitude (nonlinear) Q measurements to studies of high amplitude seismic pulse propagation in the near field.

1. Forced Resonant Vibrations - Q can be calculated using the formula

$$Q = \frac{f_R}{\Delta f}$$

where f_R is the resonant frequency, measured at peak amplitude, and Δf is the bandwidth of the peak, measured at half-power amplitude. It is well established (cf. Nowick and Berry, 1972) that this is a sound technique for measuring Q in a material with linear response. However, this may not be a particularly satisfactory technique for measuring energy dissipation in a material with properties that depend on vibration amplitude. In most rocks, when vibrations exceed the elastic limit the modulus decreases with increasing vibration amplitude (Mavko, 1979; Tittmann, 1983). This is probably due to frictional sliding along micro-

cracks, a nonlinear and nonrecoverable process. The shape of the resonance peak at low amplitude is nearly symmetrical. At high amplitudes the peak becomes severely skewed toward the high frequency side. This effect, illustrated in Fig. 3.2 for natural dome salt at 0.68 MPa effective pressure, is a result of the decrease in modulus with increasing vibration amplitude, and has been observed at high amplitudes in all but the most tightly consolidated rock types. This result casts suspicion on the usefulness of the swept forced resonance technique for obtaining reliable measurements of Q and modulus at high nonlinear amplitudes.

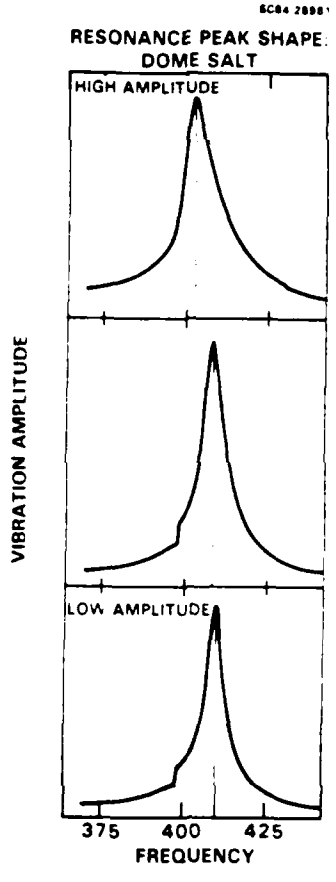

Fig. 3.2

Resonance curve shapes at various strain amplitudes. Low amplitude vibrations within the linear regime are generally nearly symmetric, as shown in the lower frame. Skewness is apparent at higher nonlinear amplitudes (center and top frames).

2. Homogeneity of Strain - Another problem with measuring nonlinear Q involves the variation in strain amplitude throughout the specimen. In the previous study (Tittmann, 1983) we reported measurements of Q as a function of strain amplitude, which was calculated at a position of maximum strain in the specimen. In these measurements first-order strains varied from zero to the value actually reported for both torsional and flexural vibrations, depend-

ing on location within the specimen. Maximum strain amplitude is defined for torsion and flexure in Figs. 3.3 and 3.4, respectively. Minster and Day (1985) discuss this issue in more detail and estimate the magnitude of its effect on the attenuation-amplitude curves.

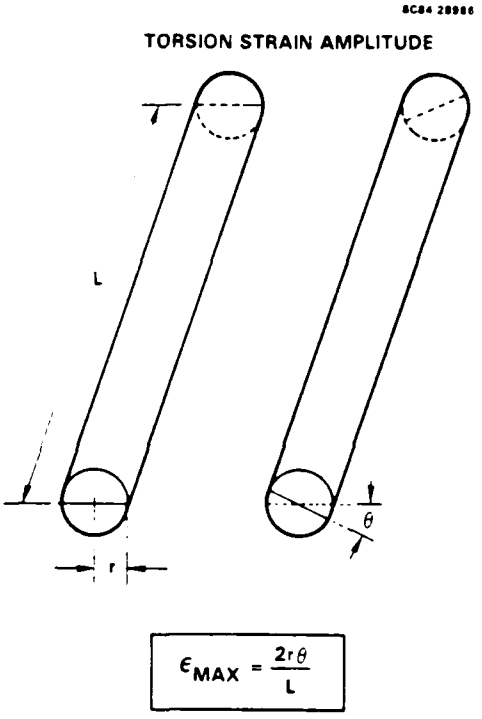

Fig. 3.3 Definition of strain amplitude in torsion.

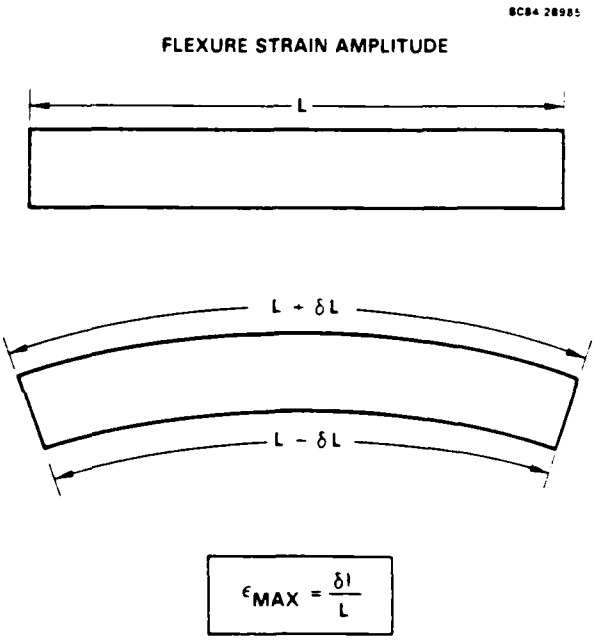

Fig. 3.4 Definition of strain amplitude in flexure.

3. Tension vs Compression - During both extensional and flexural resonances each increment of volume within the specimen is subjected to tensile stresses half of the time and to compressive stresses the other half. A tacit assumption is that the material behaves the same in compression as it does in tension. The apparent drop in bar modulus with increasing vibration amplitude

has been noted previously (Tittmann, 1983), and is probably also related to the distortion of the resonance peak shape with increasing strain. It has not been proven, however, whether either the frictional losses or the effective modulus of a rock are the same in tension as they are in compression. Resonating bar-type measurements are not capable of resolving the details of the rheological response of materials to nonlinear loading.

3.2 Quasi-Static Stress-Strain Analysis

On the basis of the above discussion it is evident that the laboratory work most beneficial to resolving the issue of linearity vs nonlinearity would involve studies of the mechanical response of various test site materials, including salt, to realistic seismic pulse loading histories. Such studies would necessarily require the application of true uniaxial strain while test specimens are subjected simultaneously to a hydrostatic bias stress. This type of study is very difficult technically, and results of such studies do not exist, at least not in the open literature. Several papers have examined the details of stress-strain hysteresis loops under nonlinear, uniaxial stress loading conditions (distinguished from uniaxial strain) (Gordon and Davis, 1968; McKavanagh and Stacey, 1974), but in each of these cases only compressional measurements were performed.

In this program we have examined the effects of combined high amplitude tensile and compressive uniaxial loading stress on four different rock types: Westerly granite, Boise sandstone, Berea sandstone, and Indiana limestone, under ambient pressure conditions. This represents the first stage of a new effort with the ultimate goal to examine the mechanical response of test site materials, including dome salt, to high amplitude uniaxial strain loading at elevated hydrostatic pressures. The details of the stress-strain hysteresis loops are studied in order to determine whether loss is related to intergranular friction or to linear anelastic relaxation. The response of the rock to compressive loading is compared with that of tensile loading.

4.0 MECHANICAL RESONANCE STUDIES

We have examined the response of Westerly granite to sinesoidal loading using flexural and torsional resonances. The measurements clearly define the amplitude of transition from linearity to nonlinearity at elevated effective pressures. The results are compared with previous measurements of dome salt under similar conditions.

4.1 Experimental Techniques

The techniques used for resonance measurements are essentially the same as those described previously (Tittmann, 1983). Briefly, a cylindrical specimen of Westerly granite, 13 cm long and 0.71 cm radius, was clamped into an apparatus used to force flexural and torsional vibrations. In this particular study the resonant frequency was between 500 and 550 Hz for all measurements. The Q of the resonance was calculated from the ratio of the resonant frequency to the bandwidth of the resonance curve. The voltage applied to the electromagnetic transducer used to drive the resonance was varied in order to affect the amplitude of the vibration. Thus, attenuation and RMS driving voltage were measured as a function of vibration amplitude in the sample. Provided that the sample behaves linearly, the attenuation should be independent of vibration amplitude, and the RMS driving voltage should be proportional to vibration amplitude (c.f. Tittmann, 1983). Measurements were made in both wet and dry Westerly granite at effective pressures from 0 to 34 MPa.

4.2 Experimental Results

The results of this study are shown in Figs. 4.1 through 4.20. They are qualitatively consistent with the results of previous studies of natural dome salt (Tittmann, 1983) in that linear behavior is observed at all low amplitudes, with a transition to nonlinear behavior at high strain. The transition amplitude is near 10^{-6} in all cases, including both torsion and flexure, regardless of water content, increasing very slightly with increasing effective pressure.

SC5361.10FR

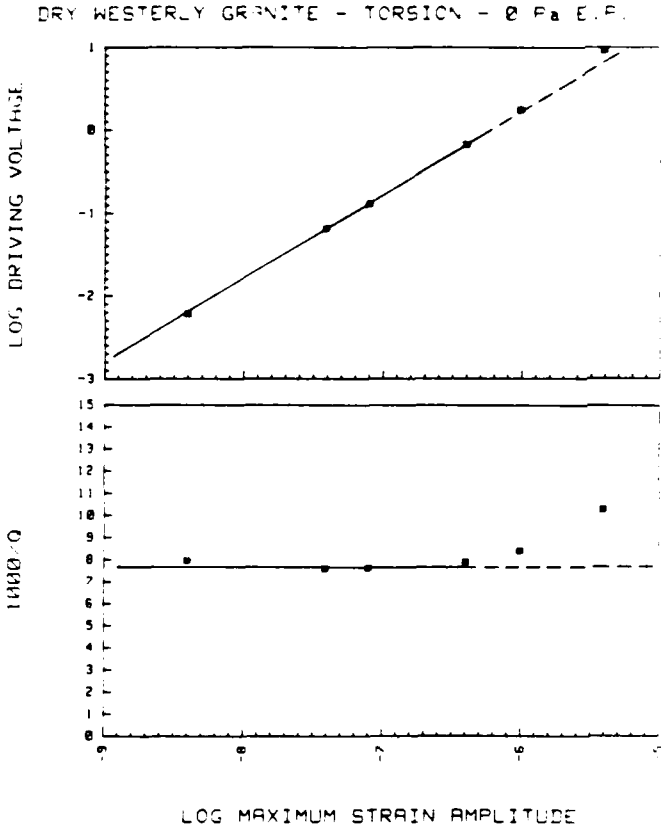

Fig. 4.1

Attenuation and log RMS driving transducer voltage as a function of maximum strain amplitude for torsional vibrations in dry Westerly granite at 0 MPa effective pressure.

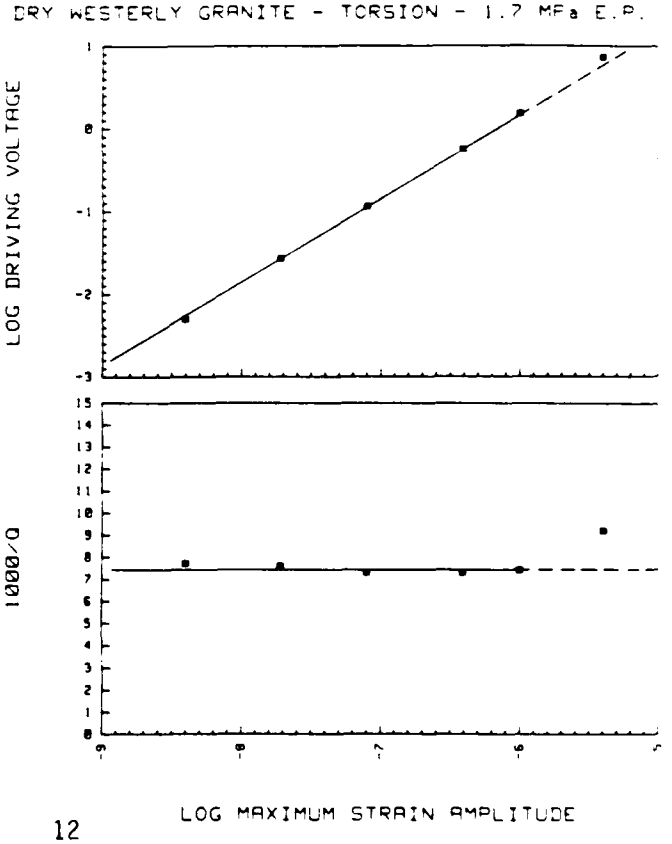

Fig. 4.2

Attenuation and log RMS driving transducer voltage as a function of maximum strain amplitude for torsional vibrations in dry Westerly granite at 1.7 MPa effective pressure.

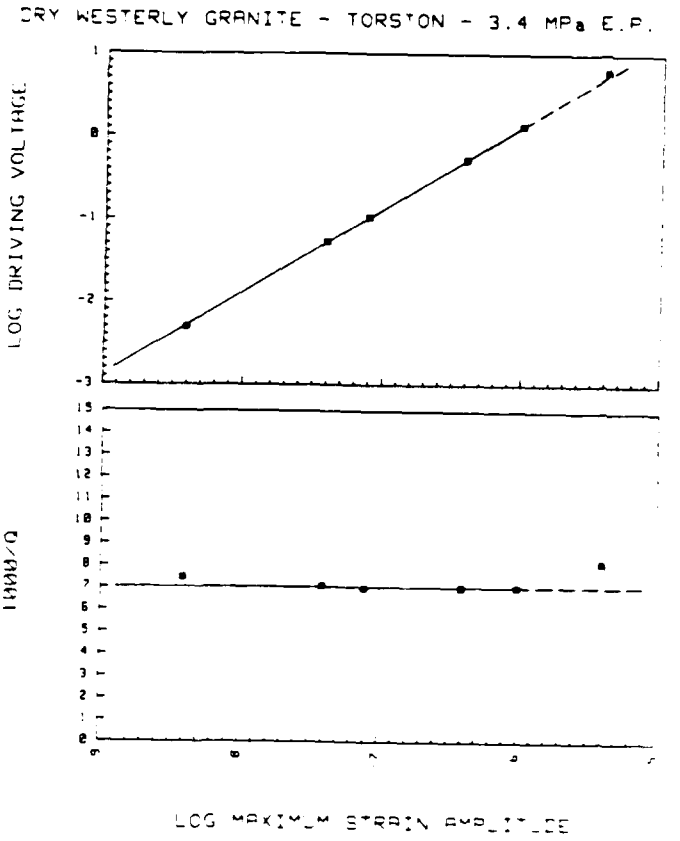

Fig. 4.3

Attenuation and log RMS driving transducer voltage as a function of maximum strain amplitude for torsional vibrations in dry Westerly granite at 3.4 MPa effective pressure.

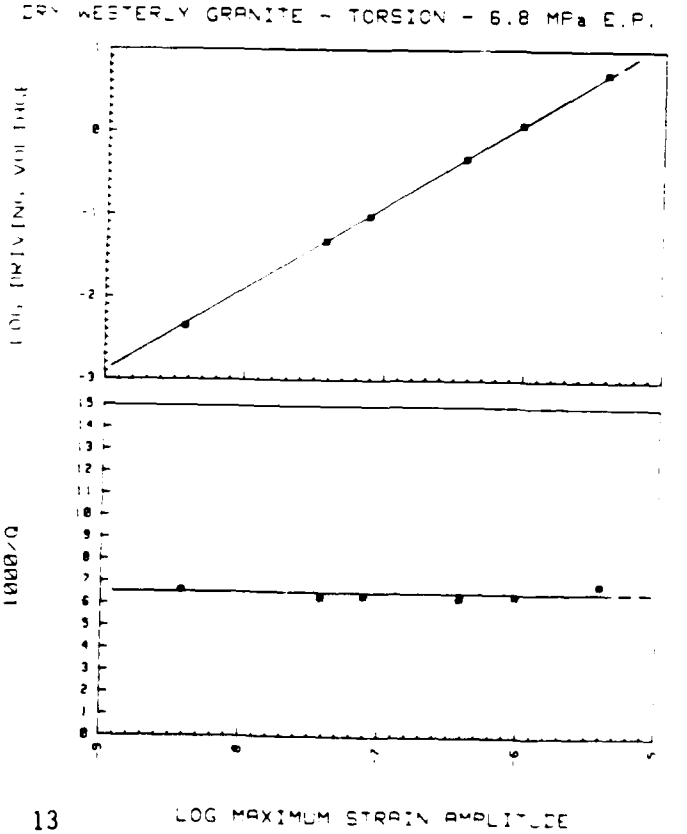

Fig. 4.4

Attenuation and log RMS driving transducer voltage as a function of maximum strain amplitude for torsional vibrations in dry Westerly granite at 6.8 MPa effective pressure.

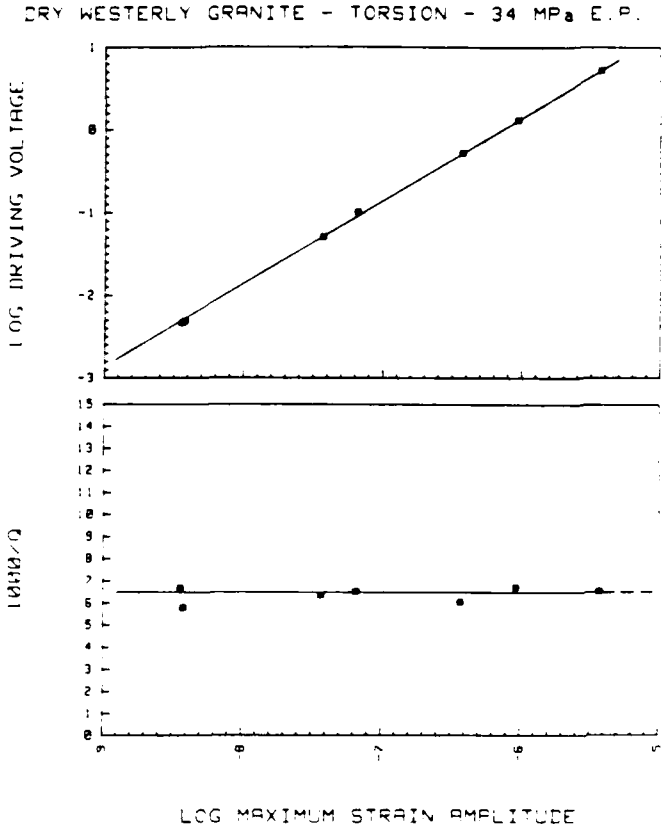

SC5361.10FR

Fig. 4.5

Attenuation and log RMS driving transducer voltage as a function of maximum strain amplitude for torsional vibrations in dry Westerly granite at 34 MPa effective pressure.

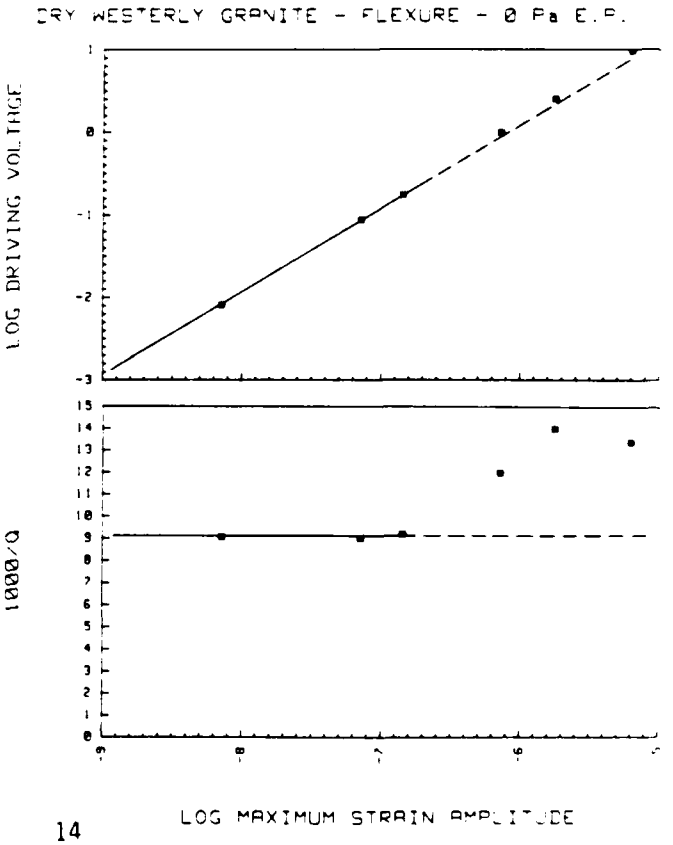

Fig. 4.6

Attenuation and log RMS driving transducer voltage as a function of maximum strain amplitude for flexural vibrations in dry Westerly granite at 0 MPa effective pressure.

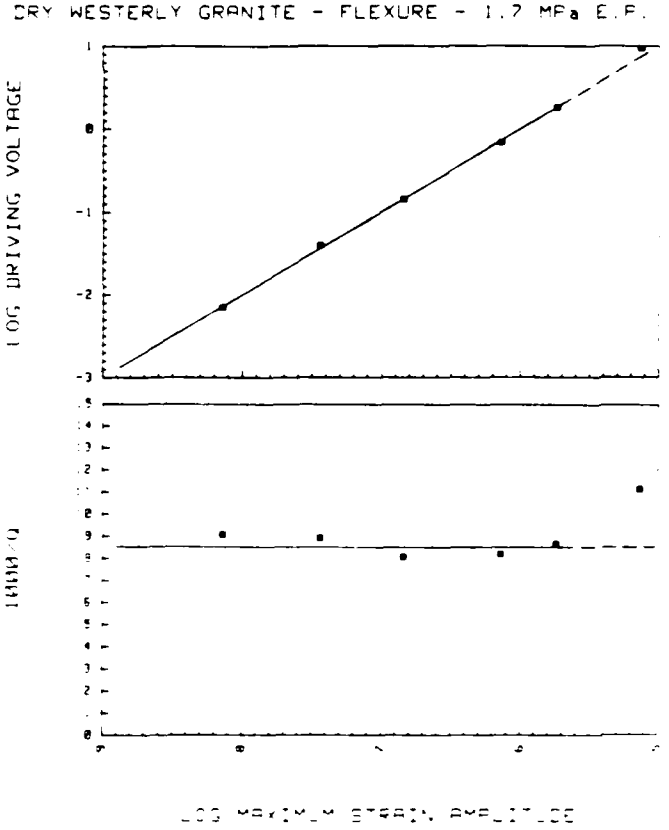

SC5361.10FR

Fig. 4.7

Attenuation and log RMS driving transducer voltage as a function of maximum strain amplitude for flexural vibrations in dry Westerly granite at 1.7 MPa effective pressure.

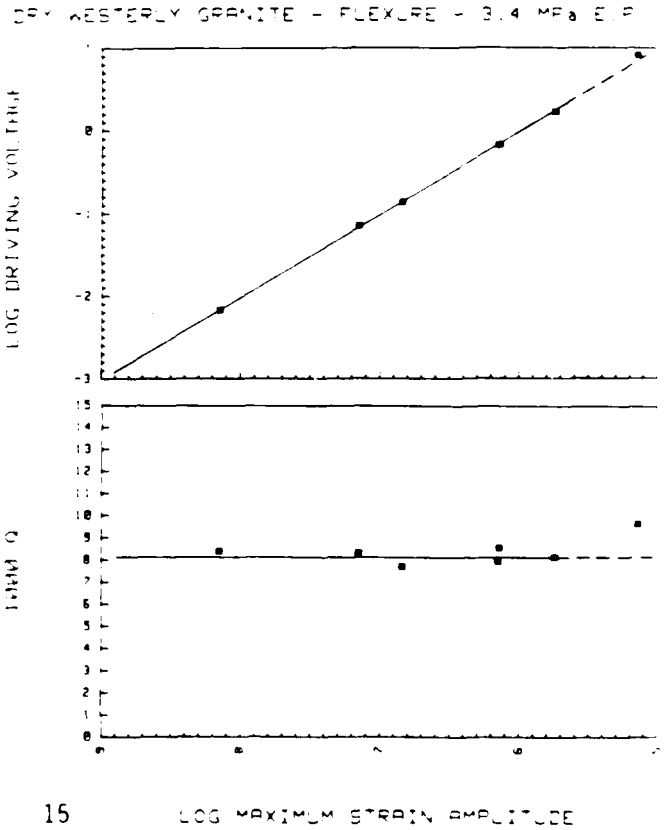

Fig. 4.8

Attenuation and log RMS driving transducer voltage as a function of maximum strain amplitude for flexural vibrations in dry Westerly granite at 3.4 MPa effective pressure.

SC5361.10FR

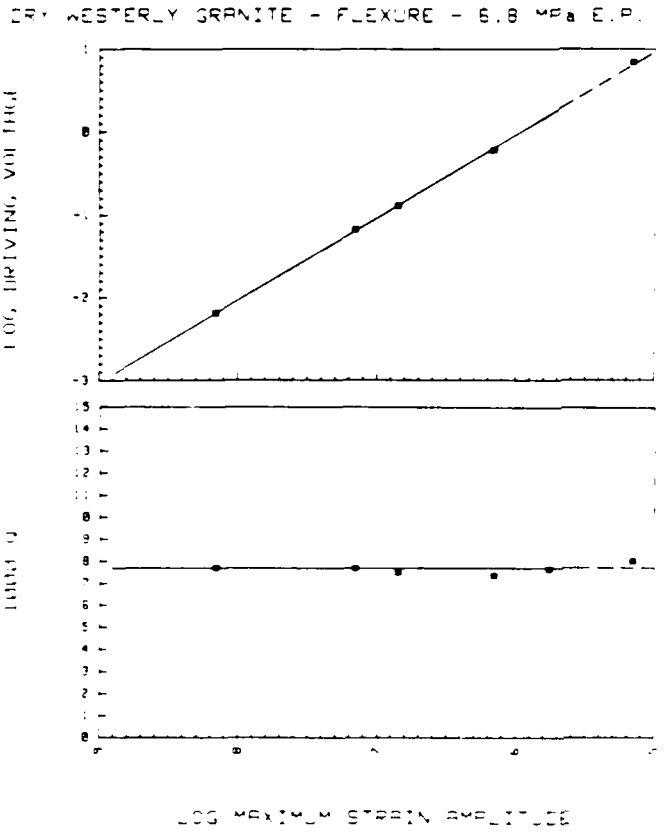

Fig. 4.9

Attenuation and log RMS driving transducer voltage as a function of maximum strain amplitude for flexural vibrations in dry Westerly granite at 6.8 MPa effective pressure.

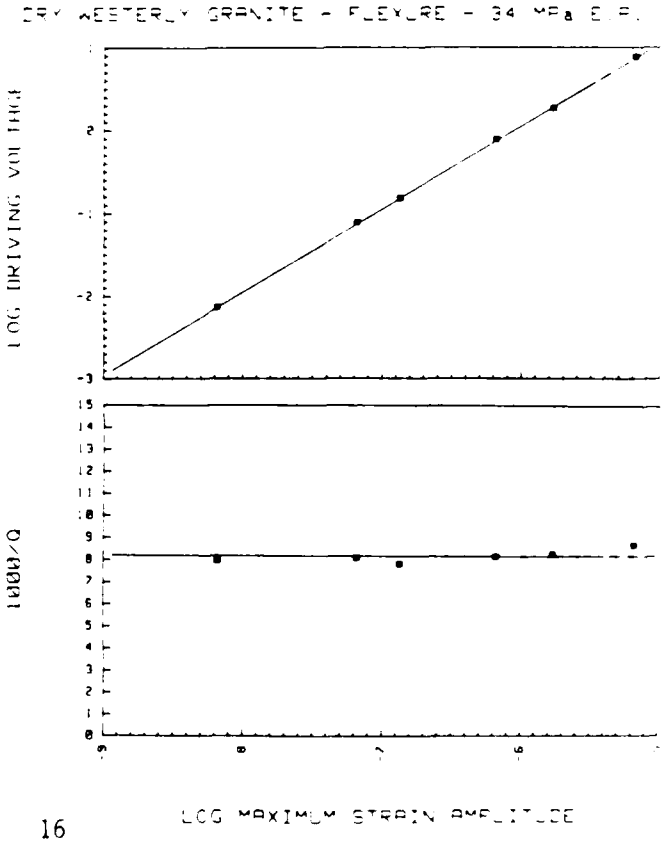

Fig. 4.10

Attenuation and log RMS driving transducer voltage as a function of maximum strain amplitude for flexural vibrations in wet Westerly granite at 34 MPa effective pressure.

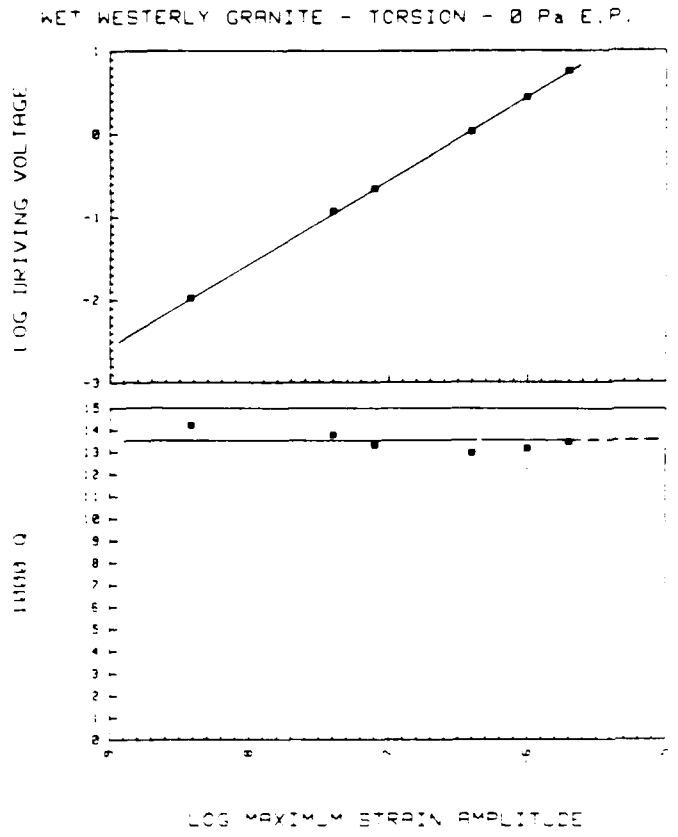

Fig. 4.11

Attenuation and log RMS driving transducer voltage as a function of maximum strain amplitude for torsional vibrations in wet Westerly granite at 0 MPa effective pressure.

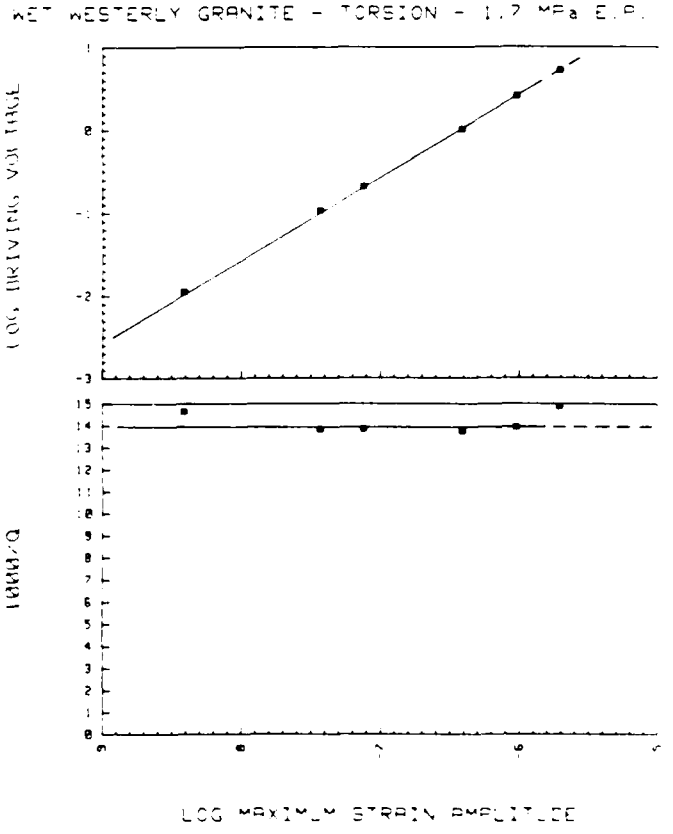

Fig. 4.12

Attenuation and log RMS driving transducer voltage as a function of maximum strain amplitude for torsional vibrations in wet Westerly granite at 1.7 MPa effective pressure.

SC5361.10FR

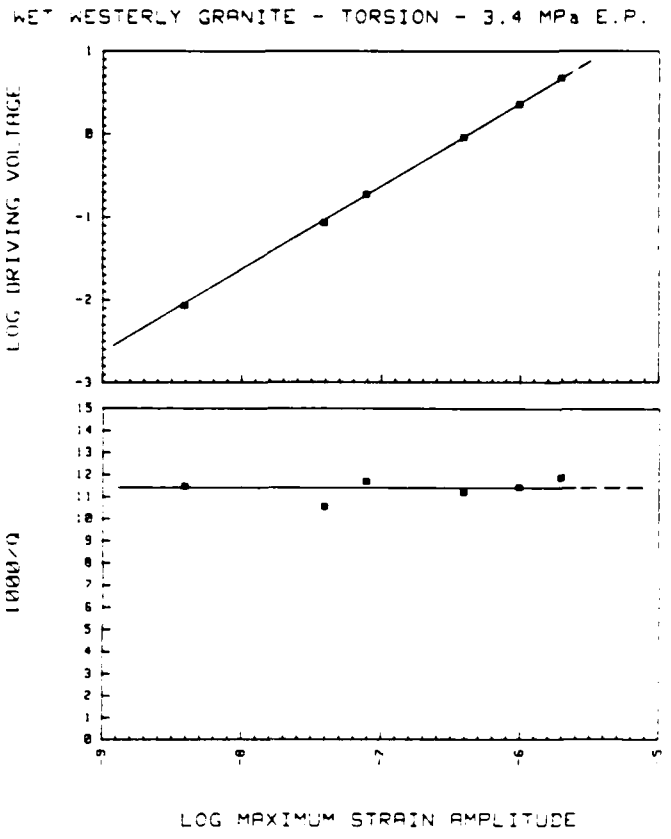

Fig. 4.13

Attenuation and log RMS driving transducer voltage as a function of maximum strain amplitude for torsional vibrations in wet Westerly granite at 3.4 MPa effective pressure.

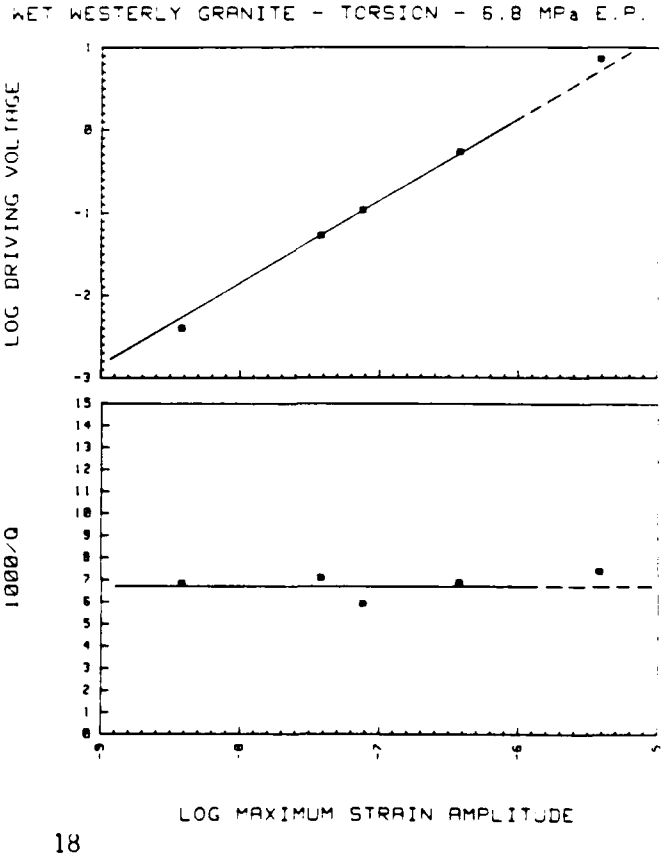

Fig. 4.14

Attenuation and log RMS driving transducer voltage as a function of maximum strain amplitude for torsional vibrations in wet Westerly granite at 6.8 MPa effective pressure.

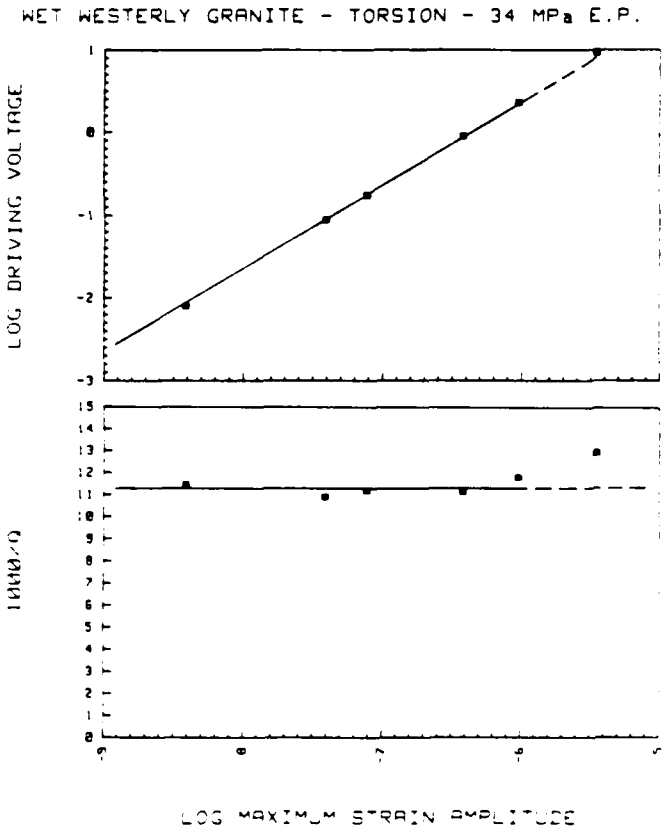

Fig. 4.15

Attenuation and log RMS driving transducer voltage as a function of maximum strain amplitude for torsional vibrations in wet Westerly granite at 34 MPa effective pressure.

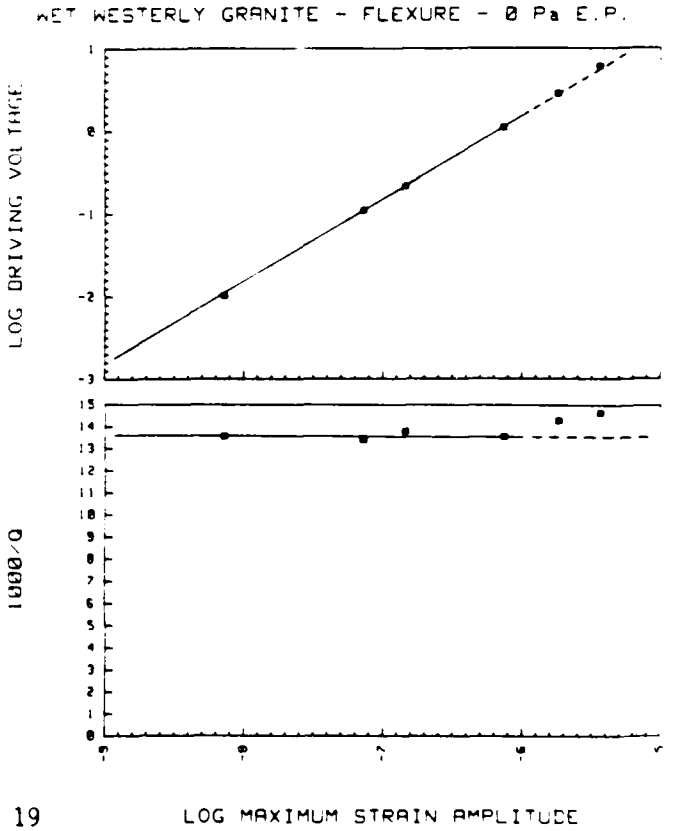

Fig. 4.16

Attenuation and log RMS driving transducer voltage as a function of maximum strain amplitude for flexural vibrations in wet Westerly granite at 0 MPa effective pressure.

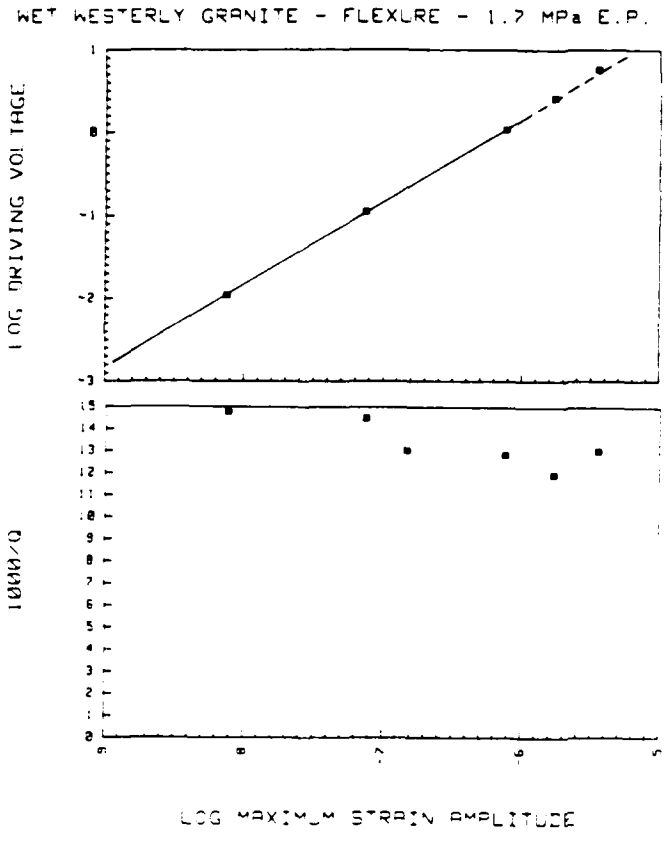

Fig. 4.17

Attenuation and log RMS driving transducer voltage as a function of maximum strain amplitude for flexural vibrations in wet Westerly granite at 1.7 MPa effective pressure.

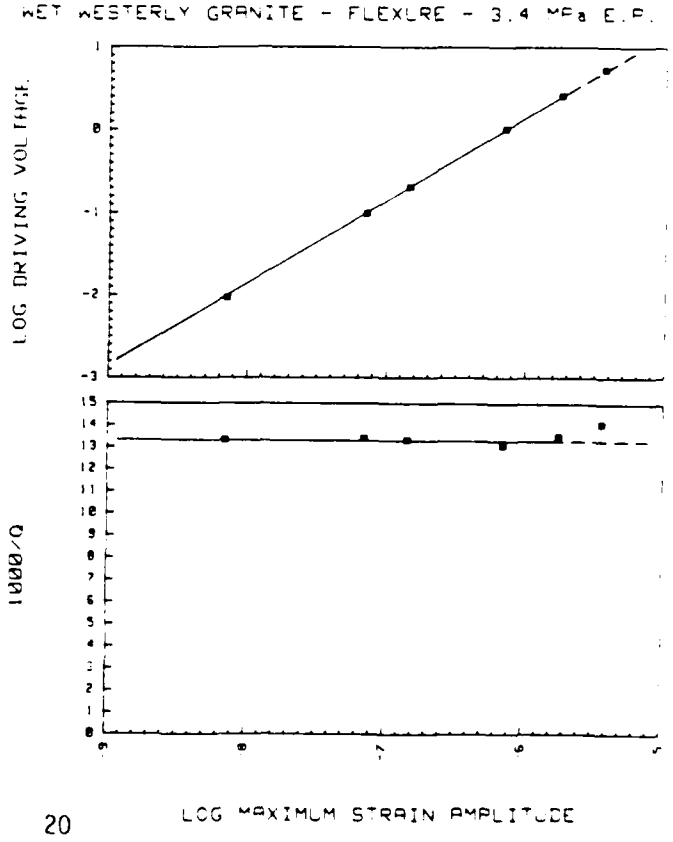

Fig. 4.18

Attenuation and log RMS driving transducer voltage as a function of maximum strain amplitude for flexural vibrations in wet Westerly granite at 3.4 MPa effective pressure.

SC5361.10FR

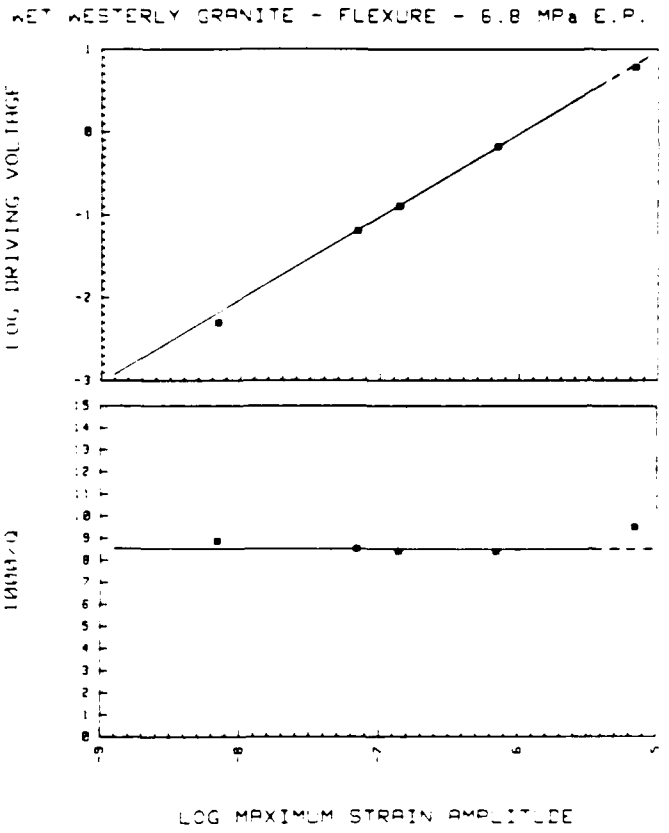

Fig. 4.19

Attenuation and log RMS driving transducer voltage as a function of maximum strain amplitude for flexural vibrations in wet Westerly granite at 6.8 MPa effective pressure.

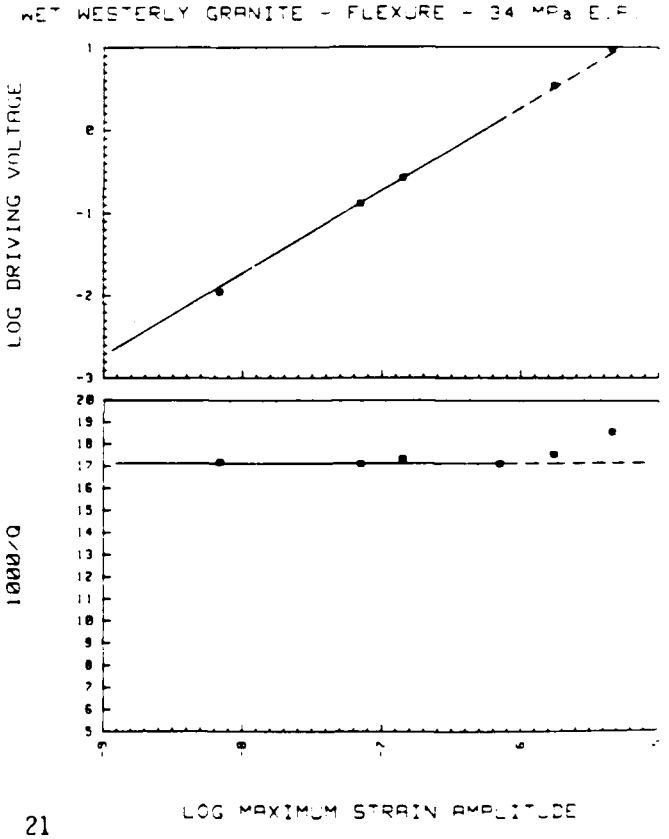

Fig. 4.20

Attenuation and log RMS driving transducer voltage as a function of maximum strain amplitude for flexural vibrations in wet Westerly granite at 34 MPa effective pressure.

5.0 QUASI-STATIC STRESS-STRAIN ANALYSIS

5.1 Experimental Techniques

Figure 5.1 includes schematic illustrations of the mechanical parts of the system used for measurement. Briefly, cylindrical rock specimens 2.54 cm in diameter and 6.35 cm long were cut from larger blocks of material. A resistance-type strain gauge was bonded to the surface of each specimen to respond to strains in the longitudinal direction. The rock was then bonded adhesively to stainless steel mounting fixtures using a semiplastic polymer resin (Crystal Bond #509, Aremco Products) that is quite brittle and stiff at room temperature, but that softens readily at approximately 70°C. By keeping the specimen warm while mounting it in the apparatus, residual stresses could be removed. Measurements were made at room temperature and under ambient pressure conditions.

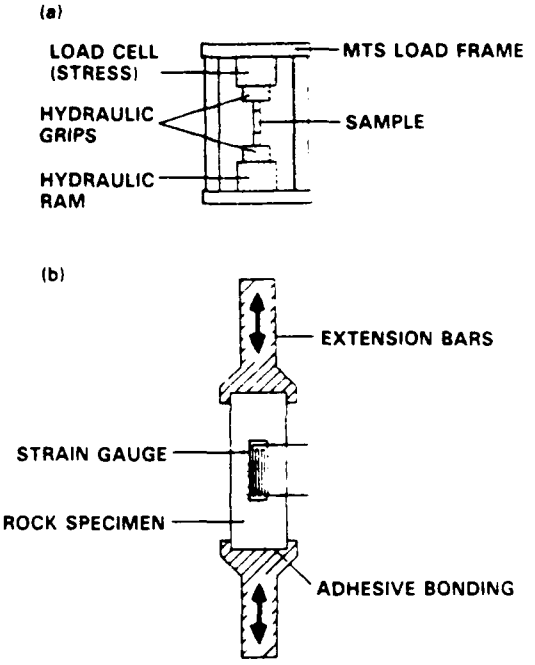

Fig. 5.1 Schematic illustration of the apparatus used for the measurement of stress-strain response curves. (a) MTS electro-(a) MTS electro-hydraulic load frame and (b) detail of sample and end fixtures.

Experiments were run using an MTS electro-hydraulic, closed-loop load frame equipped with the hydraulic hardware and controls necessary to apply alternating tensile and compressive loads. The instrumentation used for the measurements is illustrated in Fig. 5.2. The frequency of loading was usually 1 Hz, except for two series of measurements on Westerly granite and Berea sandstone at 0.1 Hz. A series of eight-cycle bursts of load-controlled constant strain rate

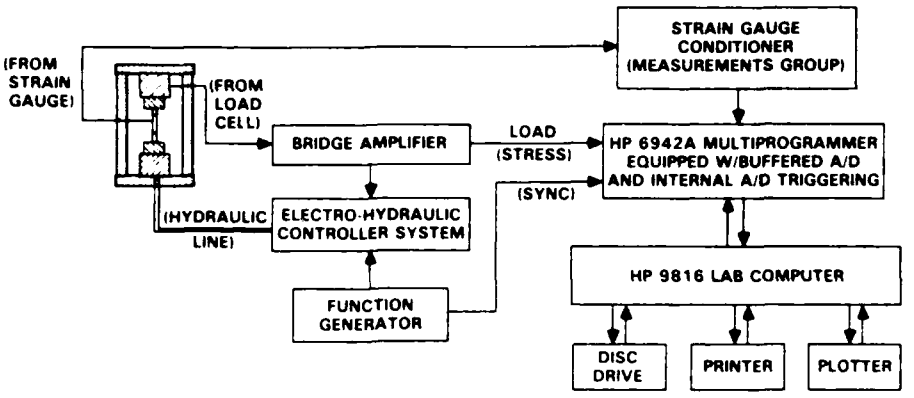

Fig. 5.2 Schematic illustration of instrumentation used to acquire and process stress-strain response curves.

triangle wave loading were applied to each specimen. Measurements of load and strain were collected simultaneously, digitized, and stored in the computer.

Representative time functions of stress and strain are illustrated in Fig. 5.3. Measurements were obtained on each sample using bursts of increasing maximum stress, starting with $\pm 3.4 \times 10^5$ Pa and working up to a maximum of $\pm 3.4 \times 10^7$ Pa, unless precluded by the breakage of the specimen. As many as 5 bursts of 8 waves each were applied at low amplitudes in order to enable satisfactory signal averaging when the signal to noise ratio was low. At higher amplitudes the signal-to-noise ratio was good, and only one eight-cycle burst was run in order to avoid excessive damage to the specimen.

5.2 Experimental Results

To test (a) the linearity of the experimental apparatus and (b) the stiffness of the adhesive bonds, the first phase of the experimental study involved measurements of stress and strain on an aluminum bar which has a relatively ideal linear elastic response. A typical curve of stress vs strain for an aluminum bar is shown in Fig. 5.4. Extensional stresses and strains are positive. Only a small amount of hysteresis is observed in this set of measurements, and it is apparent that the relationship between stress and strain is nearly linear. A small amount of hysteresis is observed and may be attributed

SC5361.10FR

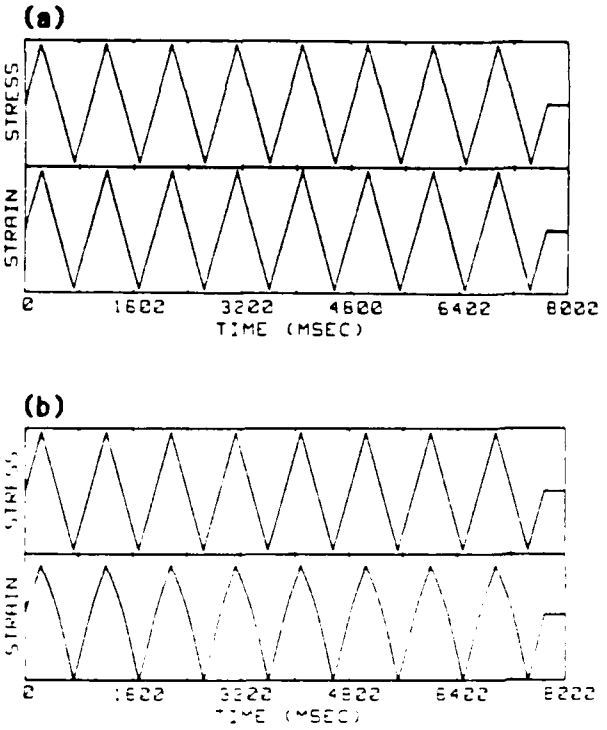

Fig. 5.3

Representative stress loading functions with corresponding strain response functions for (a) aluminum bar with a peak stress of $\pm 1.32 \times 10^7$ Pa and (b) Boise sandstone with a peak stress of 4.38×10^7 Pa.

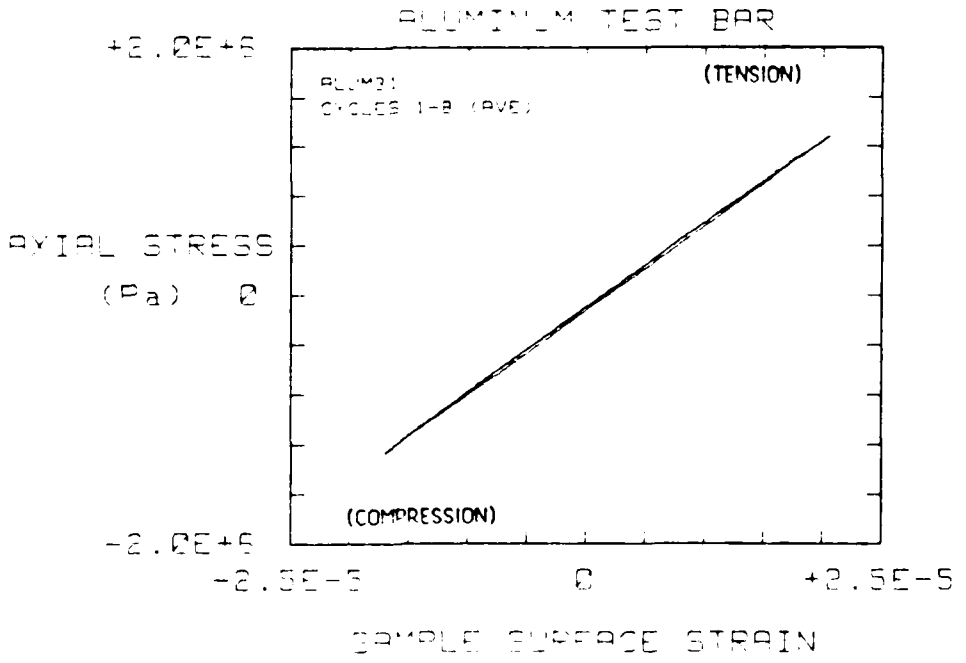

Fig. 5.4 Stress-strain response for aluminum test bar.

to plastic flow in the resin used to bond the aluminum bar to the loading fixtures. This is a relatively insignificant effect compared with the large amounts of hysteresis and nonlinearity observed in rocks under corresponding stresses.

Experimental results also show that each rock displays nearly linear behavior when the loading is very small, around 4.5×10^4 Pa, resulting in strains between 2×10^{-6} and 6×10^{-6}, depending on rock type (Figs. 5.5 through 5.8). At higher load levels (Figs. 5.9 through 5.12) there is evidence of strong nonlinearity and inelasticity in the weakest frame rock, Berea sandstone, while the nonlinear and inelastic effects are more subtle in the stronger frame rocks especially Indiana limestone. In all rock specimens except Indiana limestone the effective modulus of the rock is significantly larger in compression than in tension. In one anomalous case, Indiana limestone has a higher modulus in tension when the load is sufficiently small (Fig. 5.13).

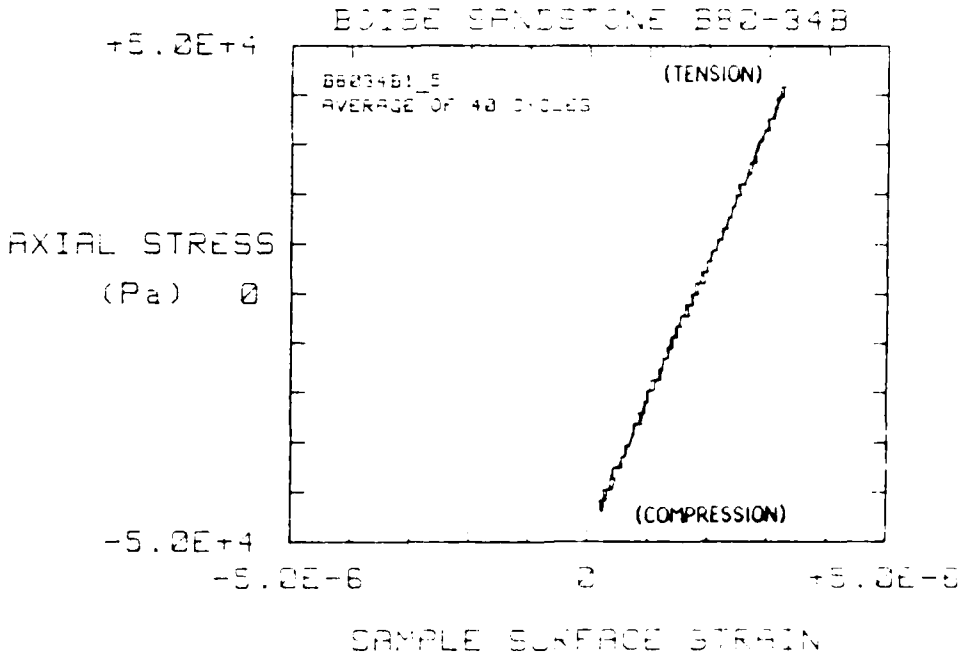

Fig. 5.5 Stress-strain response for Boise sandstone with a peak loading stress of 4.5×10^4 Pa showing nearly linear behavior.

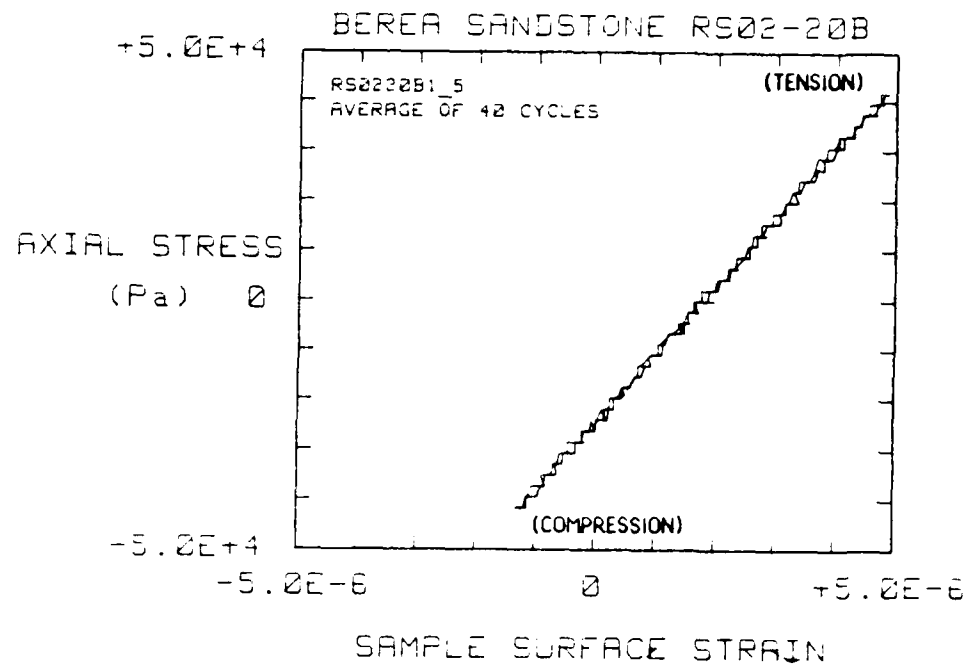

Fig. 5.6 Stress-strain response for Berea sandstone with a peak loading stress of 4.5×10^4 Pa showing nearly linear behavior.

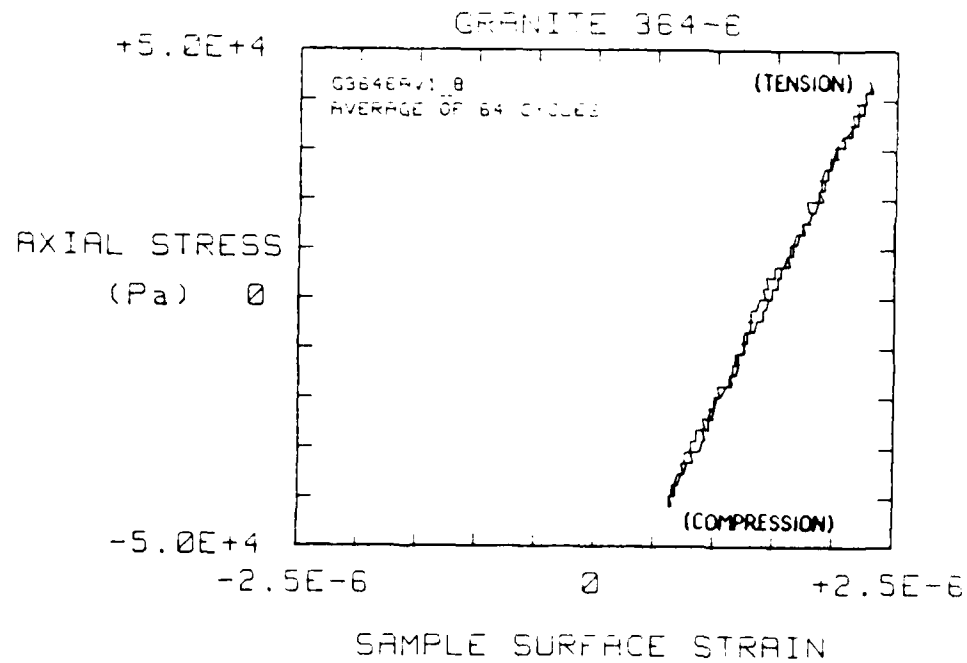

Fig. 5.7 Stress-strain response for Westerly granite with a peak loading stress of 4.5×10^4 Pa showing nearly linear behavior.

SC5361.10FR

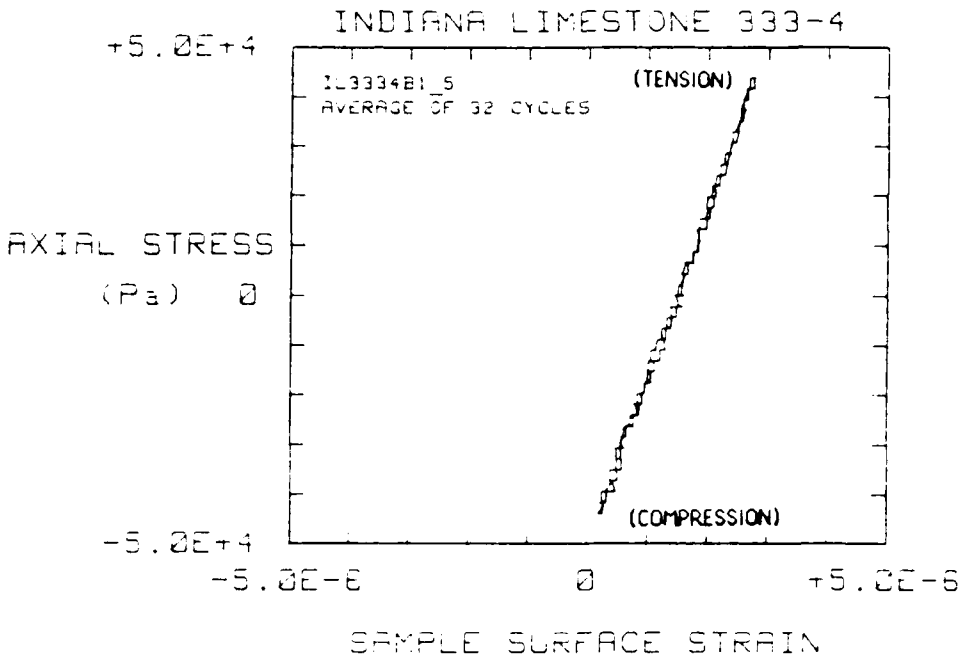

Fig. 5.8 Stress-strain response for Indiana limestone with a peak loading stress of 4.5×10^4 Pa showing nearly linear behavior.

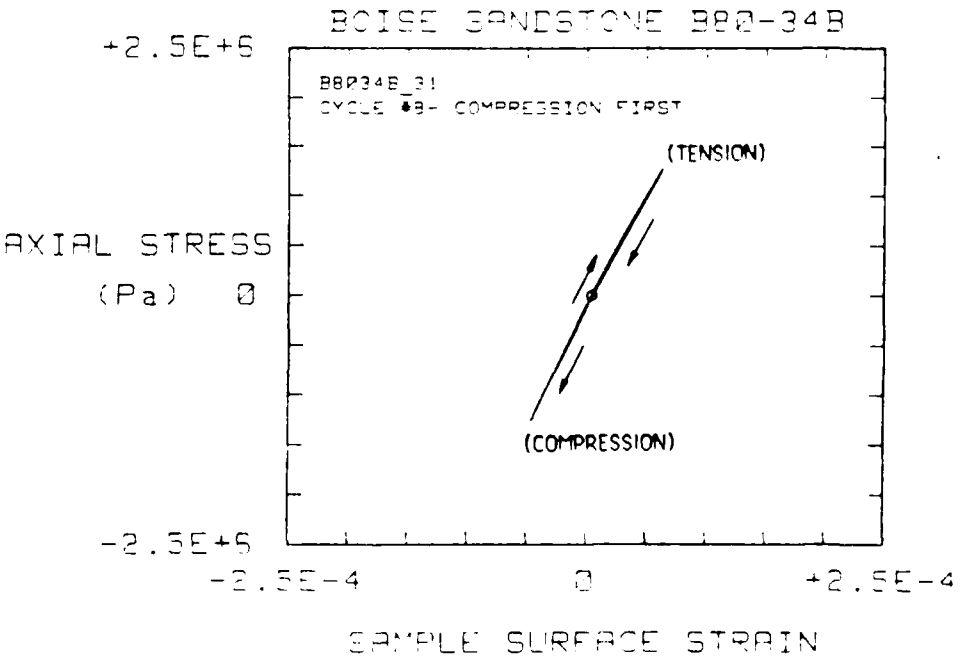

Fig. 5.9 Stress-strain response for Boise sandstone with a peak loading stress of 1.32×10^6 Pa.

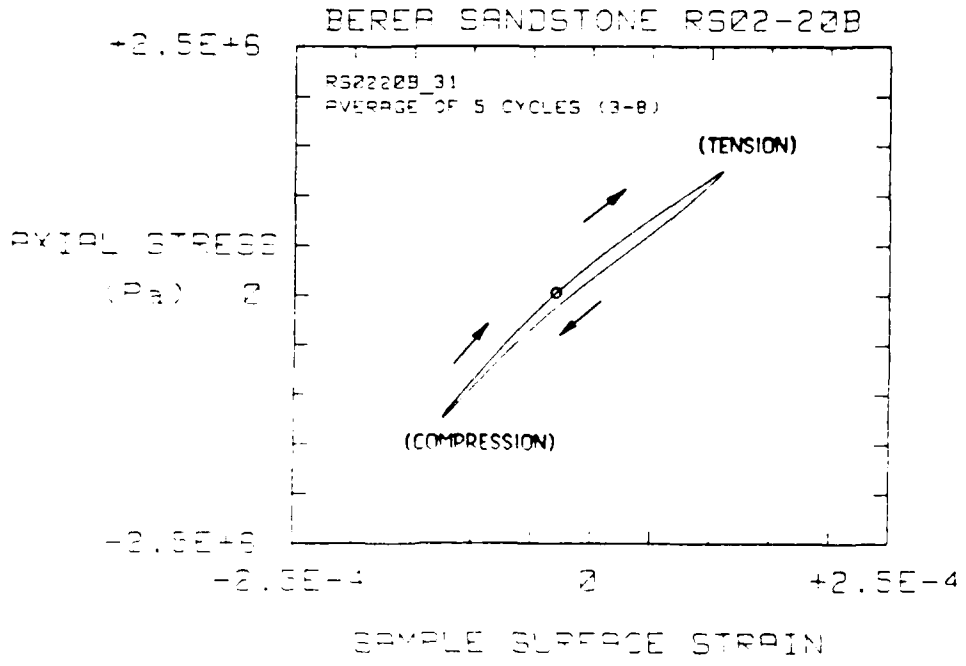

Fig. 5.10 Stress-strain response for Berea sandstone with a peak loading stress of 1.32×10^6 Pa.

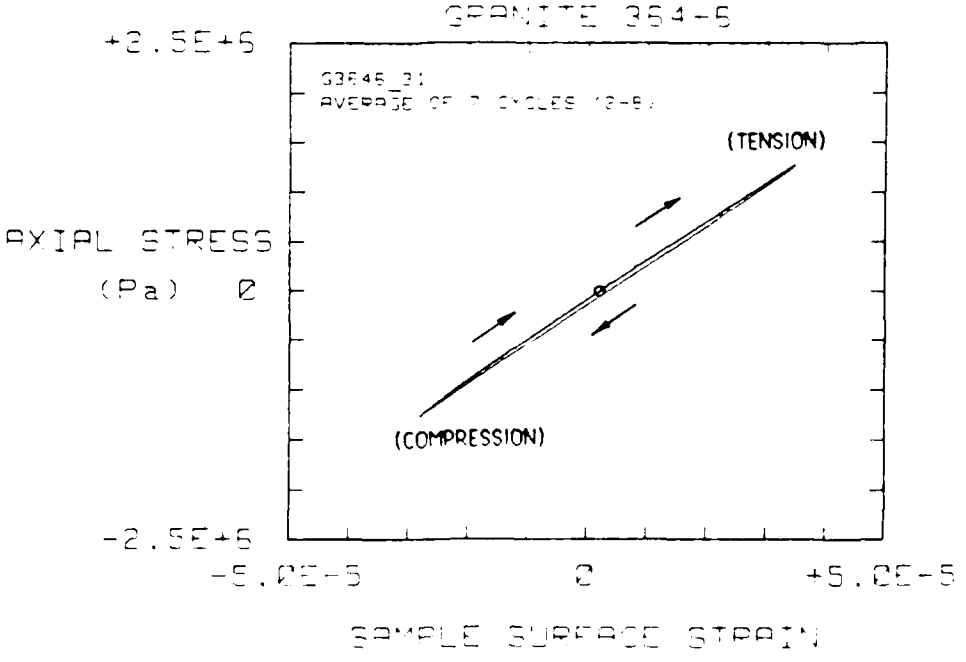

Fig. 5.11 Stress-strain response for Westerly granite with a peak loading stress of 1.32×10^6 Pa.

SC5361.10FR

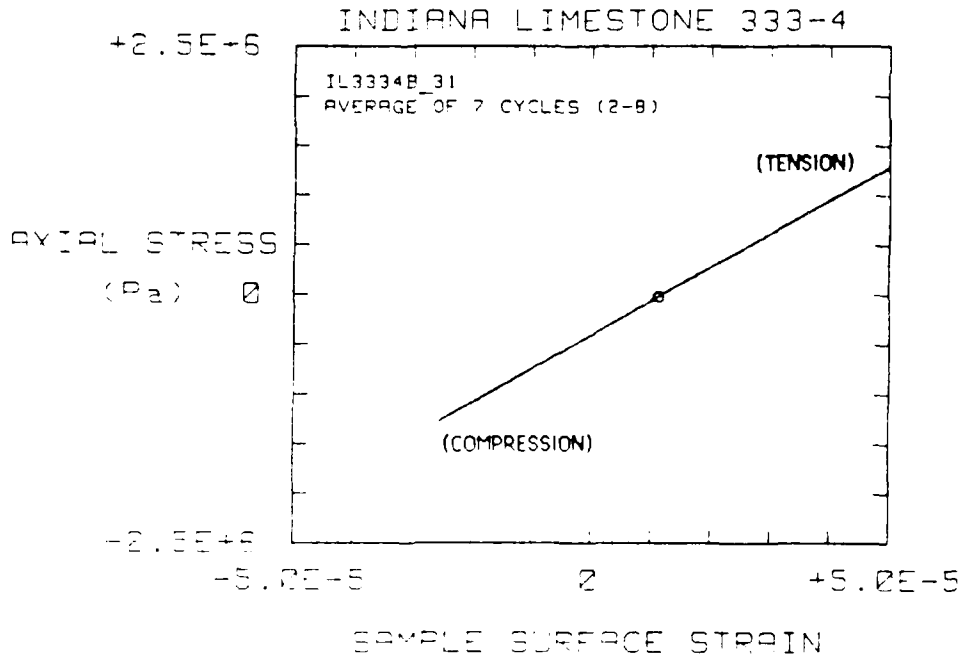

Fig. 5.12 Stress-strain response for Indiana limestone with a peak loading stress of 1.32×10^6 Pa.

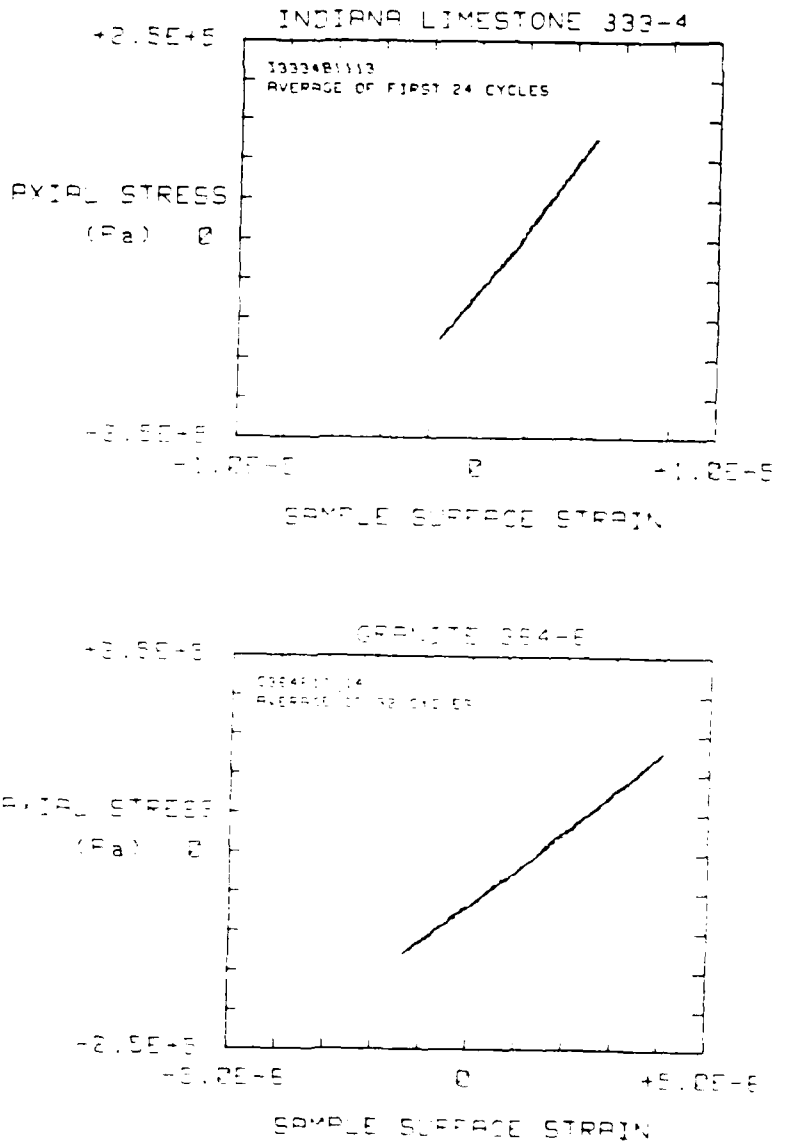

Fig. 5.13 Stress-strain response for two rocks showing the anomalous occurrence of a slightly higher effective modulus in tension than in compression. Peak loading stresses are relatively small (1.32×10^5 Pa) in each case.

McKavanagh and Stacy (1974) argue that it is possible to distinguish between linear anelastic relaxation and nonlinear relaxation, such as intergranular friction, by examining the shape of the hysteresis loop tips. Cusped tips indicate a nonlinear mechanism, while rounded tips indicate linear anelastic relaxation. Expanded views of the hysteresis loop tips measured on Westerly granite, Boise sandstone, and Berea sandstone are shown in Figs. 5.14, 5.15, and 5.16, respectively. In each case the tips are cusped and not rounded, which argues against an anelastic relaxation mechanism.

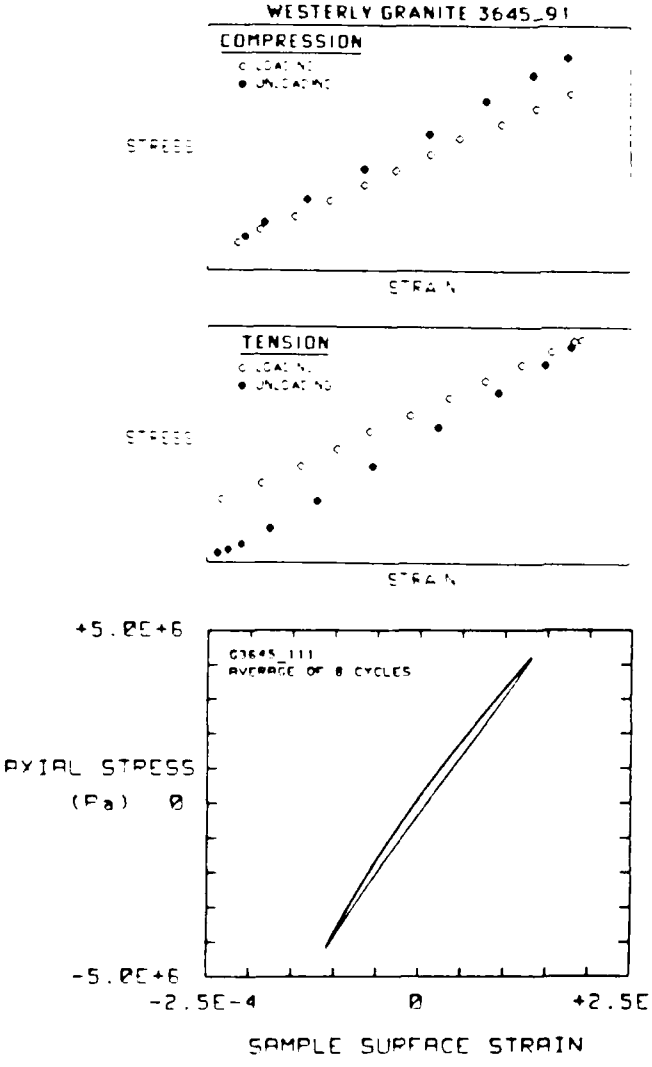

Fig. 5.14

Magnified views of the hysteresis loop tips for Westerly granite.

SC5361.10FR

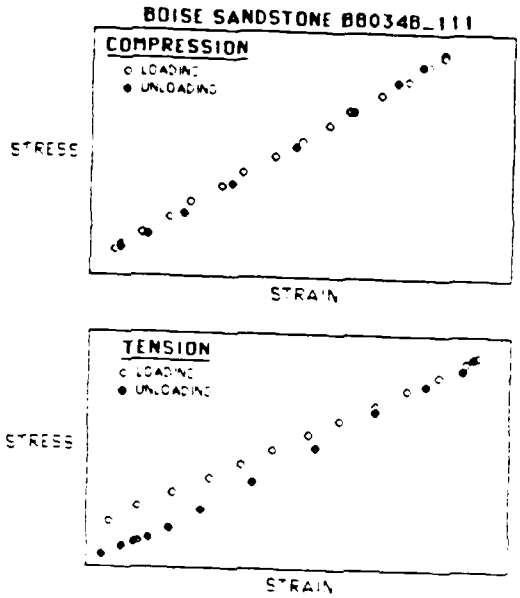

Fig. 5.15

Magnified views of the hysteresis loop tips for Boise sandstone.

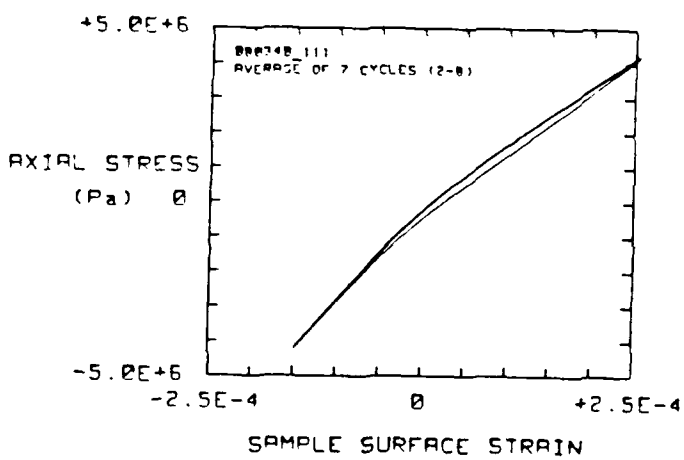

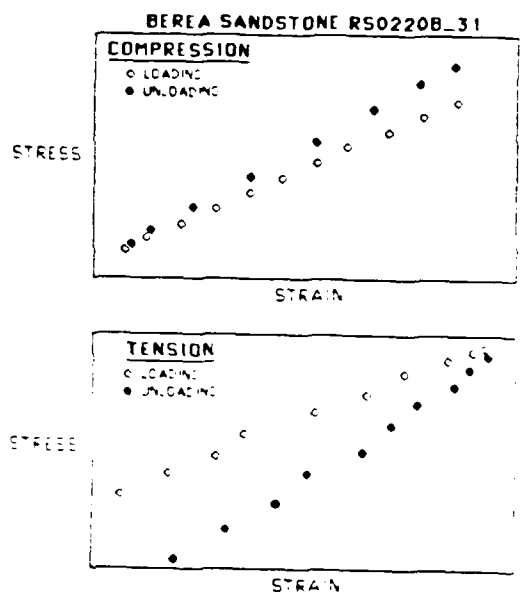

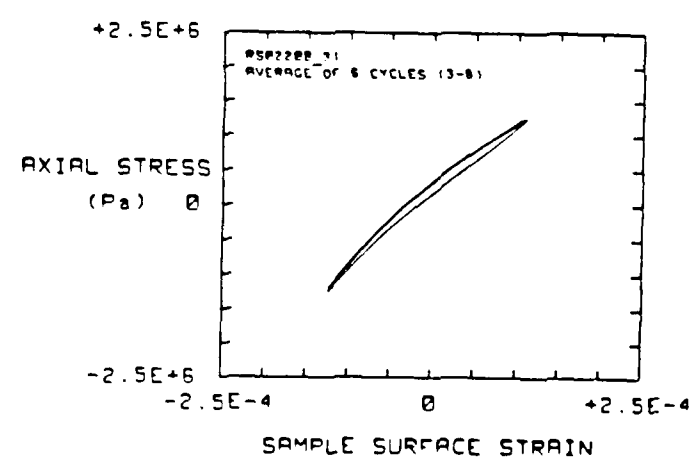

Fig. 5.16

Magnified views of the hysteresis loop tips for Berea sandstone.

In some cases there is clear evidence for large nonrecoverable changes in the rock during the first excursion to a "new" maximum load. It is reasonable to assume that these changes are associated with intergranular cracking. This is apparent when the hysteresis loop is not clearly established until at least the second cycle of loading. In the case of Berea sandstone subjected to 1.25×10^5 Pa axial stress (Fig. 5.17), the result of the first full loading cycle was a net shortening of the specimen. The nonrecoverable change at comparable stress is small in rocks with a moderately strong frame, such as Boise sandstone and Westerly granite (Figs. 5.18 and 5.19). Indiana limestone, the rock with the strongest frame, shows no hysteresis and no nonrecoverable changes after comparable loading (Fig. 5.20).

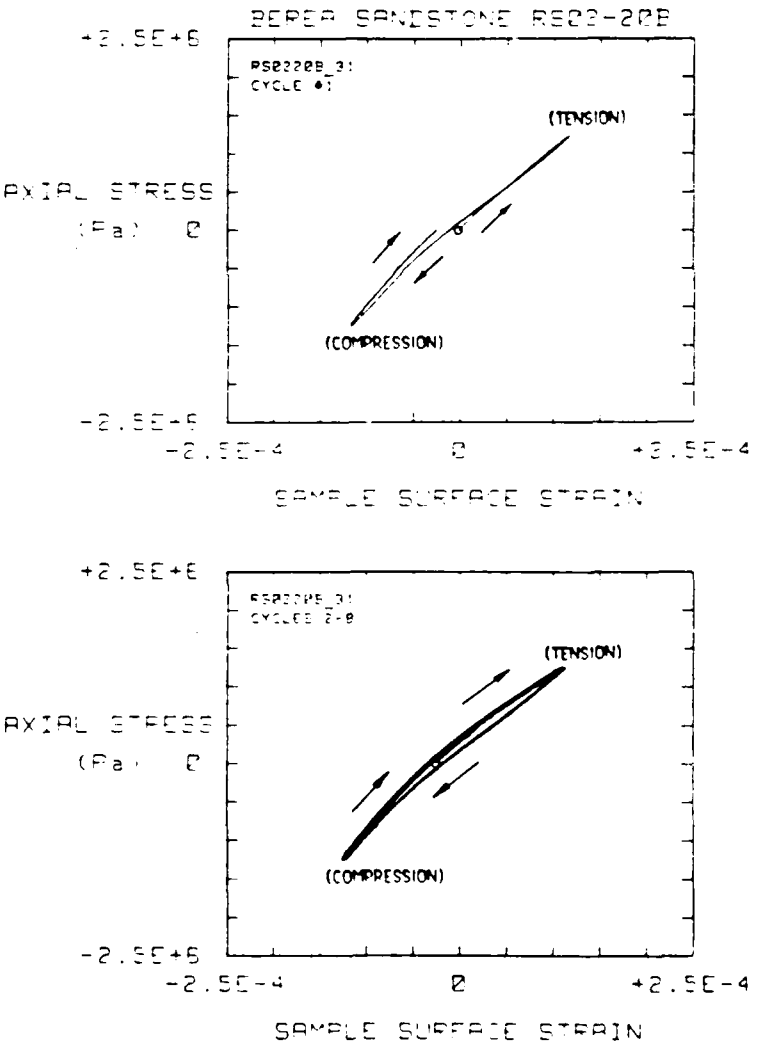

Fig. 5.17

Comparison of the first loadingcycle for Berea sandstone at 1.25×10^6 Pa with the subsequent 7 cycles showing nonrecoverable changes after the first. The previous maximum load was 4.39×10^5 Pa.

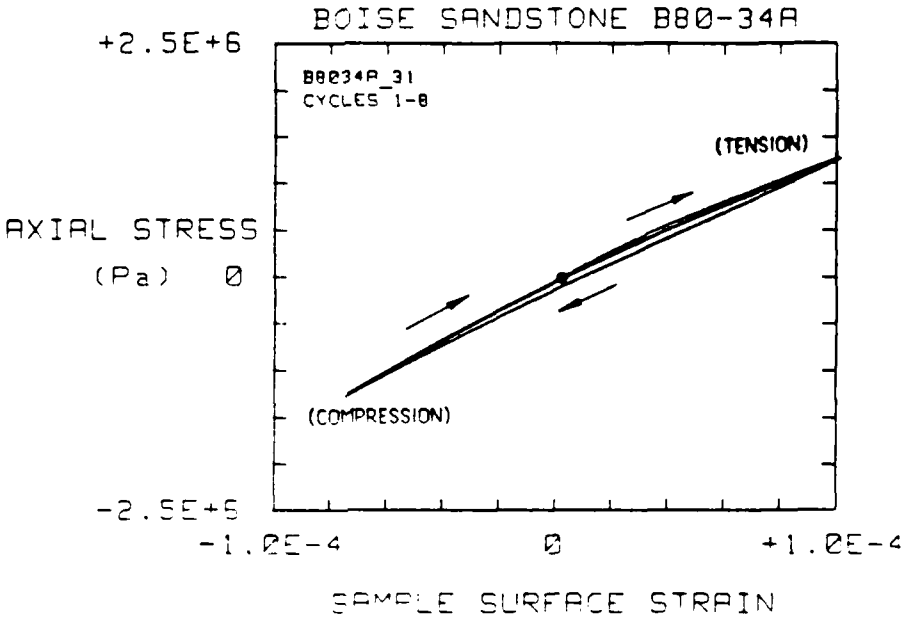

Fig. 5.18 Stress-strain response for the first eight loading cycles for Boise sandstone at 1.25×10^6 Pa. A small amount of nonrecoverable change is observed after the first cycle, but the following seven are superimposed. The previous maximum load was 4.39×10^5 Pa.

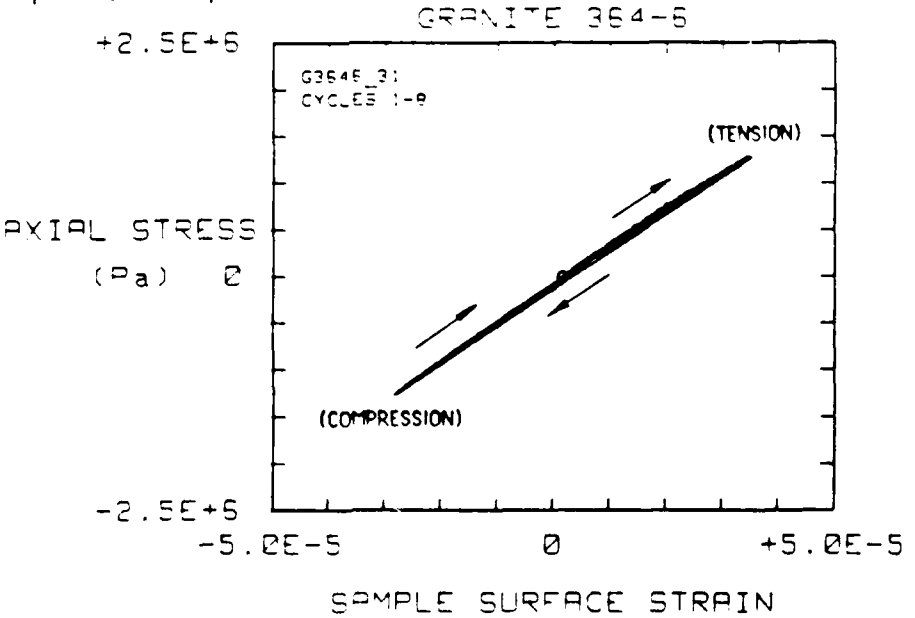

Fig. 5.19 Stress-strain response for the first eight loading cycles for Westerly granite at 1.25×10^6 Pa. A small amount of nonrecoverable change is observed after the first cycle, but the following seven are superimposed. The previous maximum load was 4.39×10^5 Pa.

SC5361.10FR

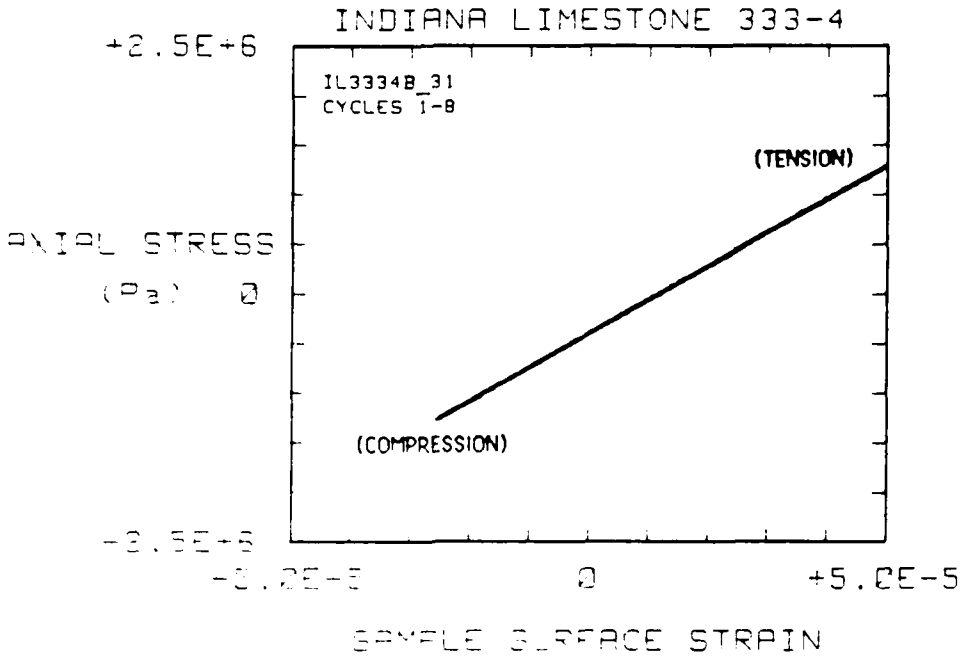

Fig. 5.20 Stress-strain response for the first eight loading cycles for Indiana limestone at 1.25×10^6 Pa. The material appears to be nearly linear elastic and nonrecoverable changes are not observed.

By reversing the direction of initial loading it is possible to examine the shape of tensional hysteresis loops and compressive hysteresis loops. In Figs. 5.21 through 5.24 we show the effects of reversing the loading direction from tension-first to compression-first, and from compression-first to tension-first, respectively, for two different rock types. It is apparent that in Boise sandstone the opening of the loop is due primarily to tensile stresses, and that the behavior in compression is nearly nonlinear elastic. In Westerly granite these effects are similar, but the contrast between compressional hysteresis and tensional hysteresis is less pronounced. A hysteresis loop exists in both compression and tension, but it is smaller in compression.

The effect of frequency on the shape of the hysteresis loop has also been examined. The results of measurements on Boise sandstone and Westerly granite at 1 Hz and at 0.1 Hz are shown in Figs. 5.25 and 5.26. The curves superimpose very well, which is consistent with a frictional relaxation mechanism, even though this evidence alone does not preclude anelastic relaxation.

SC5361.10FR

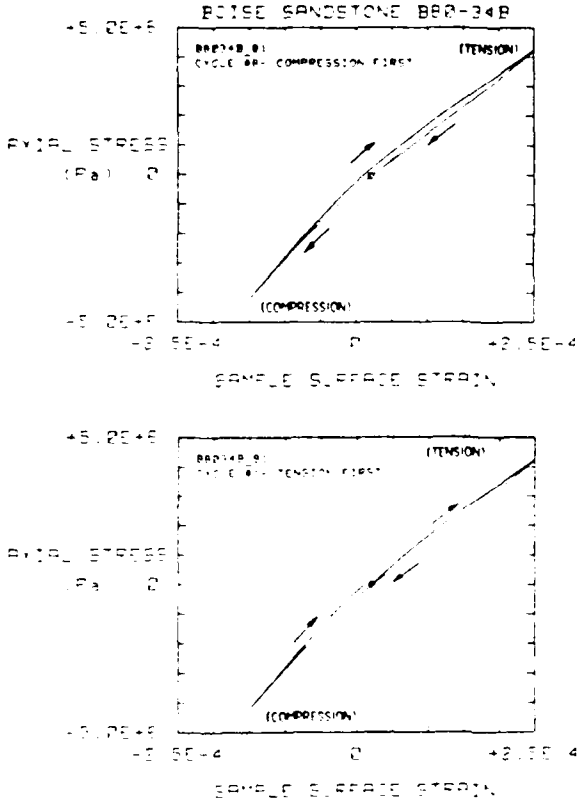

Fig. 5.21

Effect of reversing the initial loading direction from tension-first to compression-first for Boise sandstone with a maximum loading stress of 4.39×10^6 Pa, showing the lack of significant hysteresis in the compressional hysteresis loop.

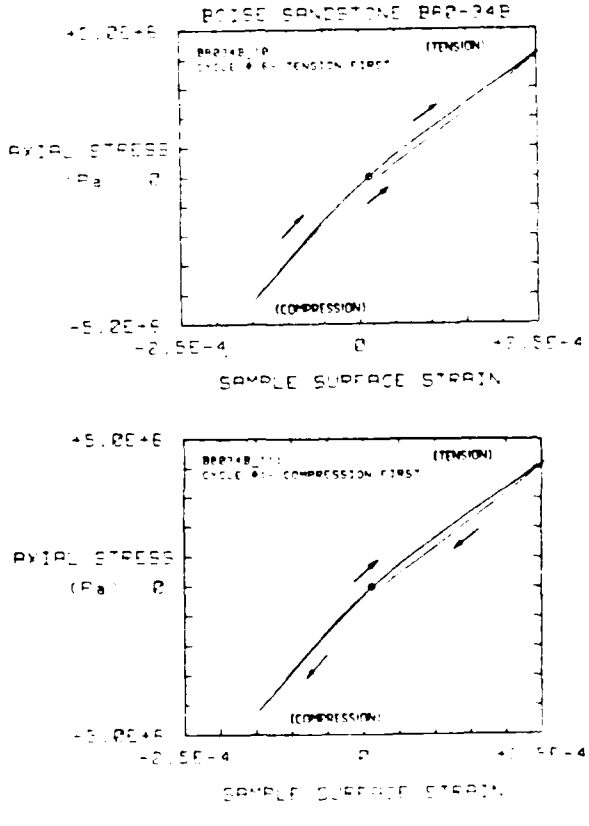

Fig. 5.22

Effect of reversing the initial loading direction from compression-first to tension-first for Boise sandstone with a maximum loading stress of 4.39×10^6 Pa, showing the development of a hysteresis loop in tension.

SC5361.10FR

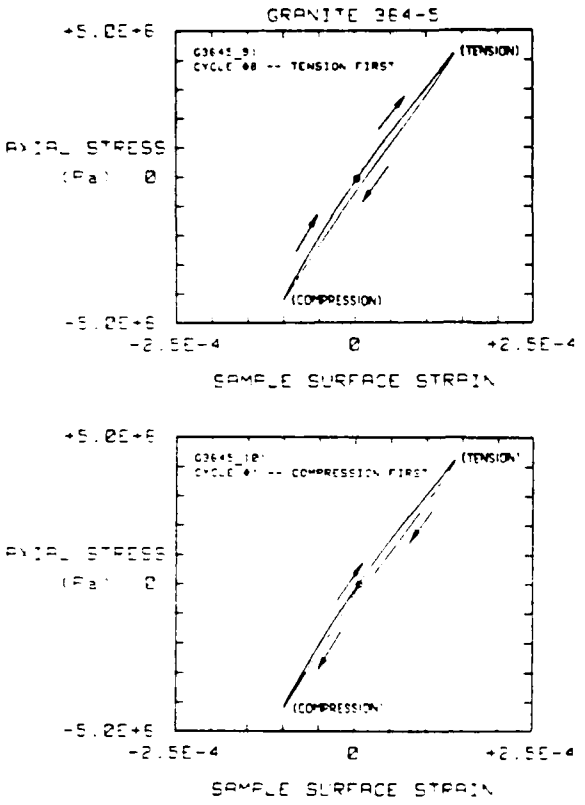

Fig. 5.23

Effect of reversing the initial loading direction from tension-first to compression-first for Westerly granite with a maximum loading stress of 4.39×10^6 Pa, showing a significant compressional hysteresis loop.

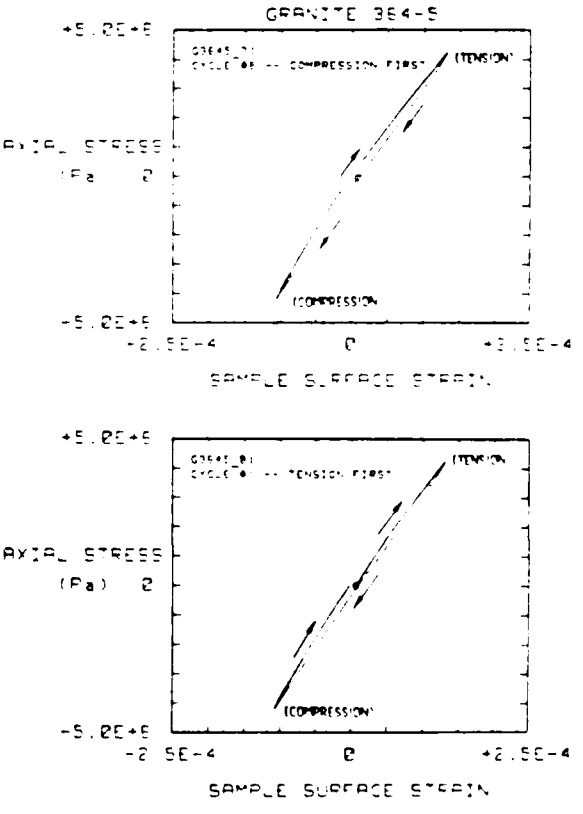

Fig. 5.24

Effect of reversing the initial loading direction from compression-first to tension-first for Westerly granite with a maximum loading stress of 4.39×10^6 Pa. Figure shows the existence of a hysteresis loop in tension which is larger than the compressional hysteresis loop illustrated in Fig. 5.23.

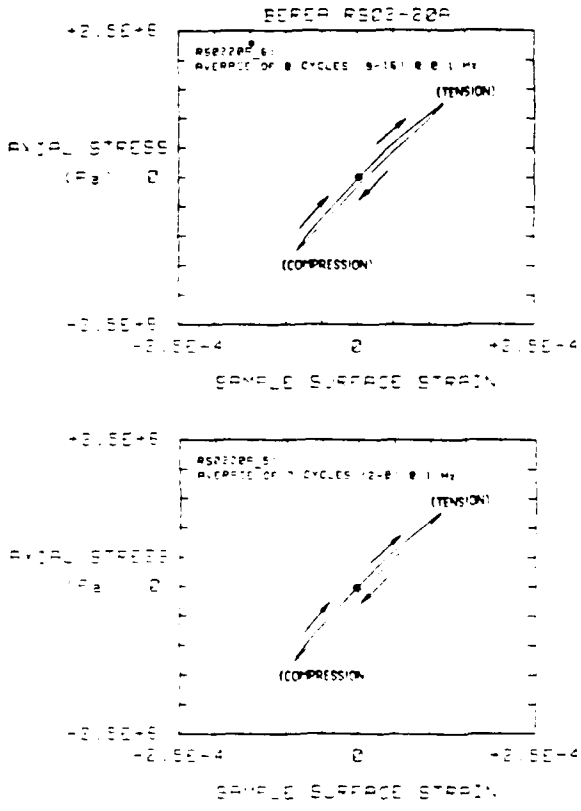

SC5361.10FR

Fig. 5.25

Comparison of the stress-strain response for Berea sandstone at two different frequencies. The traces appear to be identical.

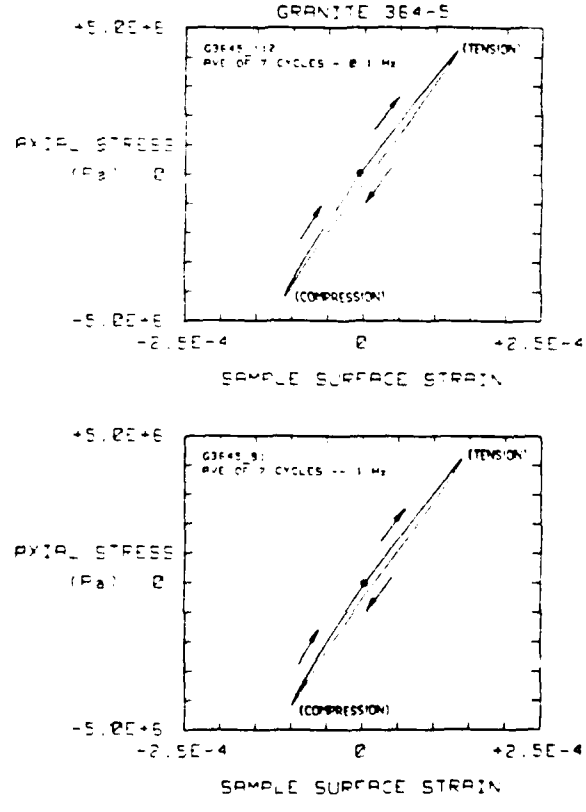

Fig. 5.26

Comparison of the stress-strain response for Westerly granite at two different frequencies. The traces appear to be identical.

Finally, we have estimated the effective attenuation from the areas under the hysteresis loops. In most cases the hysteresis loops used for these calculations were obtained using alternating compressive and tensile loading, as shown in Figs. 5.1 through 5.20. The results for all four rock types are plotted as a function of maximum strain amplitude in Fig. 5.27. In two cases it was also possible to calculate Q from hysteresis loops that represented only tensional or only compressional loading, as in Figs. 5.21 through 5.24. The results, shown in Table 5.1, show clearly that the effective attenuation in compression is significantly less than in tension, although significant differences do exist between Boise sandstone and Westerly granite.

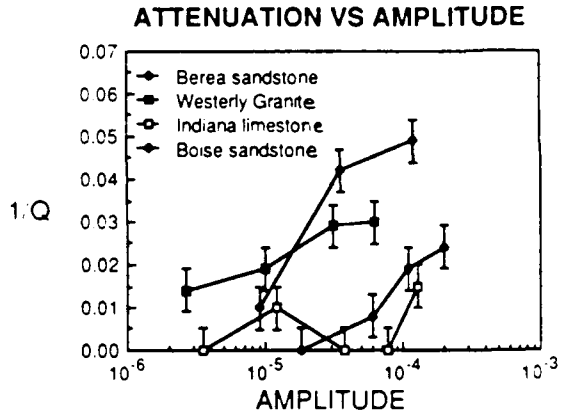

Fig. 5.27

Attenuation calculated from whole cycle hysteresis loop areas as a function of maximum strain amplitude.

Table 5.1

Estimates of Q from Hysteresis Loop Areas Measured in Tension Only, in Compression Only, and in Both Tension and Compression.

	TENSION	COMPRESSION	TENSION & COMPRESSION
WESTERLY GRANITE MAXIMUM STRAIN = 1.5 E-4	18.6	23.6	21.2
BOISE SANDSTONE MAXIMUM STRAIN = 2 E-4	22.5	200	41.8

6.0 CONCLUSIONS

We have evaluated the techniques currently in use in the laboratory for measuring the attenuation of seismic waves. We conclude that the forced swept resonance technique is best suited for measuring the Q of linear anelastic materials, and for defining the transition amplitude from linear anelastic behavior to nonlinear behavior. For evaluating losses in materials at high amplitudes, which exceed the elastic limit, the best technique requires simultaneous measurements of the time functions of stress and strain under conditions that simulate seismic loading as closely as possible.

Using the mechanical resonance approach we have studied the transition region from linearity to nonlinearity in a test specimen of Westerly granite at elevated effective pressures. Nonlinear effects in shear are observed when the maximum shear strain exceeds approximately 10^{-6}, increasing slightly with increasing effective pressure. Nonlinear effects in flexure are also observed when the strain exceeds 10^{-6}, also increasing very slightly with increasing effective pressure. These transition amplitudes probably represent a lower limit on the amplitude of transition from linear to nonlinear behavior for the compressional pulse propagating through the near-field of an explosion.

In this study we have also examined experimentally the details of stress-strain hysteresis loops when a number of different rock specimens are subjected to alternating compressive and tensile stresses. In general at nonlinear amplitudes the stiffness of the rock is greater in compression than in tension. Furthermore, preliminary results indicate that most of the energy loss during a full cycle of loading occurs as a result of strain in extension: the hysteresis loop in compression is smaller than the hysteresis loop in tension. The shape of the hysteresis loops also appear to be independent of frequency. These observations indicate a loss mechanism associated with intergranular friction. Intergranular sliding appears to be restricted by the impingement of opposing crack faces in compression, since the rock is stiffer in compression than in tension and a large hysteresis loop develops only when the rock is subjected to tensile stresses.

The results of this study indicate that the mechanical behavior of rocks can be significantly different in compression than in tension and that the onset of nonlinear effects with increasing strain may not be the same for tensile loads as for compressive loads. All available evidence indicates that the primary relaxation mechanism at nonlinear amplitudes between 10^{-6} strain and 10^{-4} strain involves intergranular friction. More experimental work in this area will shed light on the issue of linearity vs nonlinearity at intermediate strains, and also will provide realistic detailed information about rock rheology for the numerical modeling of near-field seismic pulse propagation. For this work to be most meaningful true uniaxial strain is necessary, and specimens must be exposed to elevated confining pressures.

7.0 REFERENCES

Bache, T.C., W.J. Best, R.R. Blanford, G.V. Bolin, D.G. Harkrider, E.J. Herrin, A. Ryall and M.J. Shore (1981) A Technical Assessment of Seismic Yield Estimation, DARPA Report, January 1981.

Burdick, L.J., T. Wallace and T. Lay (1984a) Modeling Near-field and Teleseismic Observations from the Amchitka Test Site, Jour. Geophys. Res., 89, 4373-4388.

Burdick, L.J., T. Lay, D.V. Helmberger and D.G. Harkrider (1984b) Implication of Records from the Spall Zone of the Amchitka Tests to Nonlinear Losses in the Source Region and to Elastic Radiation by Spall. Annual technical report for the period November 15, 1982 to November 15, 1983. Prepared for the Advanced Research Projects Agency.

Gordon, R.B. and L.A. Davis (1968) Velocity and Attenuation of Seismic Waves in Imperfectly Elastic Rock, Jour. Geophys. Res., 73, 3917-3935.

Larson, D.B. (1982) Inelastic Wave Propagation in Sodium Chloride, Bull. Seismological Soc. Amer., 72, 2107-2130.

Larson, D.B. (1984) Explosive-Induced Wave Propagation in Nugget Sandstone, Jour. Geophys. Res., 89, 9415-9424.

Mavko, G.M. (1979) Frictional Attenuation: An Inherent Amplitude Dependence, Jour. Geophys. Res., 84, 4769-4775.

McCarter, G.D. and W.R. Wortman (1985) Experimental and Analytic Characterization of Nonlinear Seismic Attenuation, Final Report for the Period March 21, 1984 through March 20, 1985. Prepared for the Advanced Research Projects Agency.

McKavanagh, B. and F.D. Stacey (1974) Mechanical Hysteresis in Rocks at Low Strain Amplitudes and Seismic Frequencies, Phys. Earth Planet. Interiors, 8, 246-250.

Minster, J.B. and S.M. Day (1985) Decay of Wavefields Near an Explosive Source Due to High-Strain, Nonlinear Attenuation, Unpublished Manuscript.

Nowick, A.S. and B.S. Berry (1972) Anelastic Relaxation in Crystalline Solids, pp. 677, Academic Press, New York.

Perret, W.R.(1967) Free-Field Particle Motion from a Nuclear Explosion in Salt, Part I, Project Dribble, Salmon Event, VUF-3012, Sandia Laboratory.

Stewart, R.R., M.N. Toksoz, and A. Timur (1983) Strain Dependent Attenuation: Observations and a Proposed Mechanism, Jour. Geophys. Res., 88, 546-554.

Tittmann, B.R. (1983) Studies of Absorption in Salt, Final Report for the period December 1, 1981 through November 30, 1982, Prepared for Air Force Office of Scientific Research.

Tittmann, B.R., M. Abdel-Gawad, C. Salvado, J. Bulau, L. Ahlberg and T.W. Spencer (1981), A Brief Note on the Effect of Interface Bonding on Seismic Dissipation, Proc. Lunar and Planetary Science Conf. 12th, 1737-1745.

Trulio, J.G. (1978) Simple Scaling and Nuclear Monitoring, Final Report of DARPA supported research program, April 1978.

Trulio, J.G. (1981) State-of-the-Art Assessment: Seismic Yield Determination, in A Technical Assessment of Seismic Yield Estimation, DARPA Report Appendix, January 1981.

Winkler, K., A. Nur and M. Gladwin (1979), Friction and Seismic Attenuation in Rocks, Nature, 227, 528-531.

END

DTIC

8—86